Eastern Hemisphere Tropical Cyclones of 1996

MARK A. LANDER

Water and Environmental Research Institute, University of Guam, Mangilao, Guam

ERIC J. TREHUBENKO

Joint Typhoon Warning Center, Nimitz Hill, Guam

CHARLES P. GUARD

Water and Environmental Research Institute, University of Guam, Mangilao, Guam

(Manuscript received 5 February 1998, in final form 30 June 1998)

ABSTRACT

This paper is an annual summary of the Eastern Hemisphere tropical cyclones of 1996. The tropical cyclone statistics presented derive from records at the Joint Typhoon Warning Center, Guam. Although the text focuses on the tropical cyclones that occurred in the western North Pacific during 1996, it also includes brief summaries of the tropical cyclones in the north Indian Ocean, south Indian Ocean, and the South Pacific. Overall, 1996 was an active year in the Eastern Hemisphere: the 28 tropical cyclones in the Southern Hemisphere were near normal, while the number of tropical cyclones in the western North Pacific and in the North Indian Ocean was above normal. The large-scale circulation anomalies typical of a cold phase (La Niña) of the El Niño–Southern Oscillation (ENSO) continued until late in the year when strong equatorial westerly winds pushed eastward. In retrospect, the return of near-normal mean monthly monsoonal flow to the tropical Pacific during November and December of 1996—punctuated by two intense equatorial westerly wind bursts—may have signaled the onset of the strong 1997 El Niño.

1. Introduction

This summary of 1996 Eastern Hemisphere tropical cyclones (TCs) was compiled from the archives of the Joint Typhoon Warning Center, Guam (JTWC). The JTWC is a joint U.S. Navy and Air Force activity with a forecast area of responsibility that extends from the 180° meridian westward to the coast of Africa, north and south of the equator. Seventy percent of the world's TCs develop in this area. The Naval Pacific Meteorology and Oceanography Command at Pearl Harbor, Hawaii, provides TC warnings for Southern Hemisphere TCs east of 180° that are included in this summary. Although the boundaries of the JTWC's area of responsibility are not strictly the boundaries of the Eastern Hemisphere, and the few TCs of the South Pacific east of the 180° meridian are included, the area covered by this summary will be referred to as the Eastern Hemisphere.

Because JTWC's main focus is on the TCs of the western North Pacific, the summary of the TCs in this basin is more detailed than are the summaries of TCs in the other basins. An extensive summary for the western North Pacific is found in section 2, which is subdivided into three topics: (a) an overview of the annual statistics coupled with a discussion of the large-scale circulation, (b) a recap of the TC activity by month, and (c) short discussions of some selected TCs. Brief summaries for the North Indian Ocean and Southern Hemisphere are found in sections 3 and 4. Concluding remarks appear in section 5.

2. Western North Pacific tropical cyclones: January–December 1996

a. Statistics and large-scale circulation

1996 produced a near-record number of significant TCs (numbered depressions and named tropical storms or typhoons) in the western North Pacific: 43 compared with 44, the record set in 1964. This number was almost 40% higher than the climatological average for the 37-yr period 1959–95 of 31 significant TCs in the western North Pacific. 1996 included six super typhoons, 15 lesser typhoons, 12 tropical storms, and 10 tropical depressions. The calendar year total of 33 tropical storms

Corresponding author address: Mark A. Lander, Water and Energy Research Institute, University of Guam, Mangilao, Guam 96923.
E-mail: mlander@uog.edu

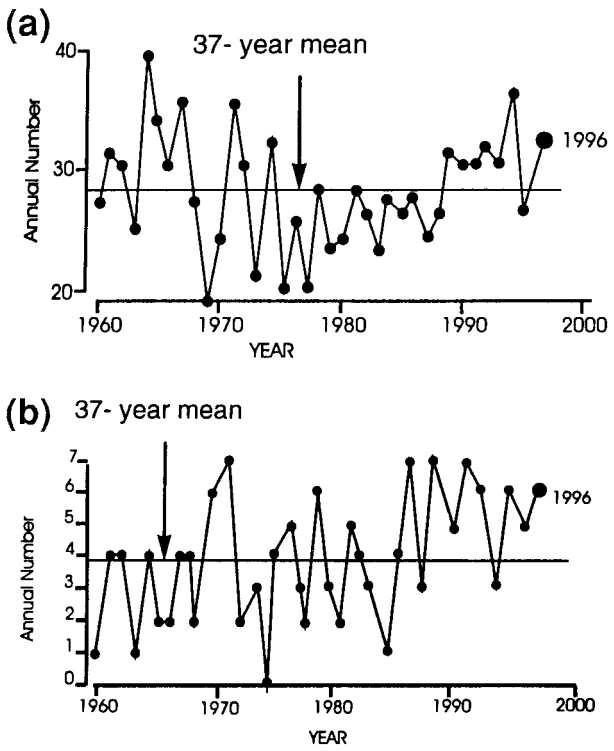

FIG. 1. (a) Tropical cyclones of tropical storm or greater intensity in the western North Pacific (1960–96). (b) Number of western North Pacific super typhoons (1960–96).

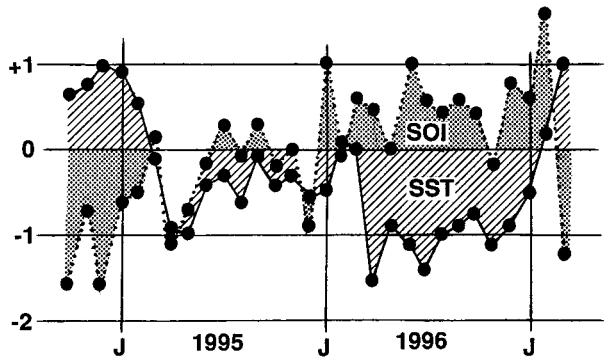

FIG. 2. Anomalies from the monthly mean for eastern equatorial Pacific Ocean SST (cross-hatched) in degrees Celsius and the SOI (shaded) for the period 1995–96. Adapted from the CPC (1996).

and typhoons was 5 above the long-term average (Fig. 1a). The calendar year total of 21 typhoons was 3 above average. Six of the typhoons became super typhoons, two more than the climatological average (Fig. 1b).

Thirty-two of the 43 significant TCs formed in the low-level monsoon trough or near-equatorial trough. Eleven—Dan (06W), Eve (07W), Joy (12W), Tropical Depression (TD) 15W, TD 17W, Piper (20W), TD 21W, Rick (22W), TD 23W, Carlo (33W), and Tropical Storm 38W—formed at relatively high latitude associated with cold-core cyclonic vortices in the tropical upper-tropospheric trough (TUTT cells). No TCs numbered or named by the Central Pacific Hurricane Center, Hawaii, or the National Hurricane Center, Miami (now known as the Tropical Prediction Center), moved into the western North Pacific from the central or eastern North Pacific during 1996.

The global climate during 1996 was characterized as a continuation of the weak cold phase of the El Niño–Southern Oscillation (ENSO) that began during 1995. Large-scale atmospheric and oceanic circulation anomalies during 1996 were generally as expected for a weak cold phase of ENSO. For example, the SST along the equator in the central and eastern Pacific was colder than normal (Fig. 2), the Southern Oscillation index (SOI) was above zero (Fig. 2), and low-level low-latitude easterly wind anomalies persisted in the western North Pacific (Fig. 3). For more details on ENSO and its effects on global climate, see Rasmusson and Carpenter (1982), Ropelewski and Halpert (1987), and Trenberth (1997).

The annual-mean genesis location is related to the status of ENSO. It tends to be east of normal during warm phase and west of normal during cold phase. As expected for a cold phase of ENSO, the annual-mean genesis location duirng 1996 was west of normal (Fig. 4a), as it was during 1995. It was also slightly north of normal. A breakdown of the genesis locations of all 1996 western North Pacific TCs (Fig. 4b) shows that most formed between 120° and 160°E. Only five formed east of 160°E, while 10—6 more than normal—formed in the South China Sea, contributing to the westward displacement of the annual-mean genesis location. Only one formed east of 160°E and south of 20°N in a region designated in Fig. 4b as the ''El Niño'' box. More TCs form in the El Niño box during El Niño (ENSO warm phase) years than during La Niña (ENSO cold phase) years (Lander 1994). During La Niña years, the few TCs that form east of 160°E typically form north of 20°N and are often directly associated with TUTT cells.

Low-level easterly wind flow was unusually persistent in the low latitudes of the western North Pacific during June–October of 1996 (Fig. 3). The normal southwest monsoon of the Philippine Sea (with its episodic extensions farther eastward) was replaced by mean monthly easterly flow. In the upper troposphere westerly wind anomalies dominated the low latitudes. Similar large-scale wind anomalies occurred during 1995, when they may have been related to a below-normal activity and a westward displacement of the mean genesis location. Despite similar wind anomalies in low latitudes, there were far more western North Pacific TCs during 1996 than during 1995. Some factors suggested for the enhanced number of TCs during 1996 include

1) frequent TUTT cell–related TCs,
2) unusual eastward penetration of the monsoon trough at high latitudes, and

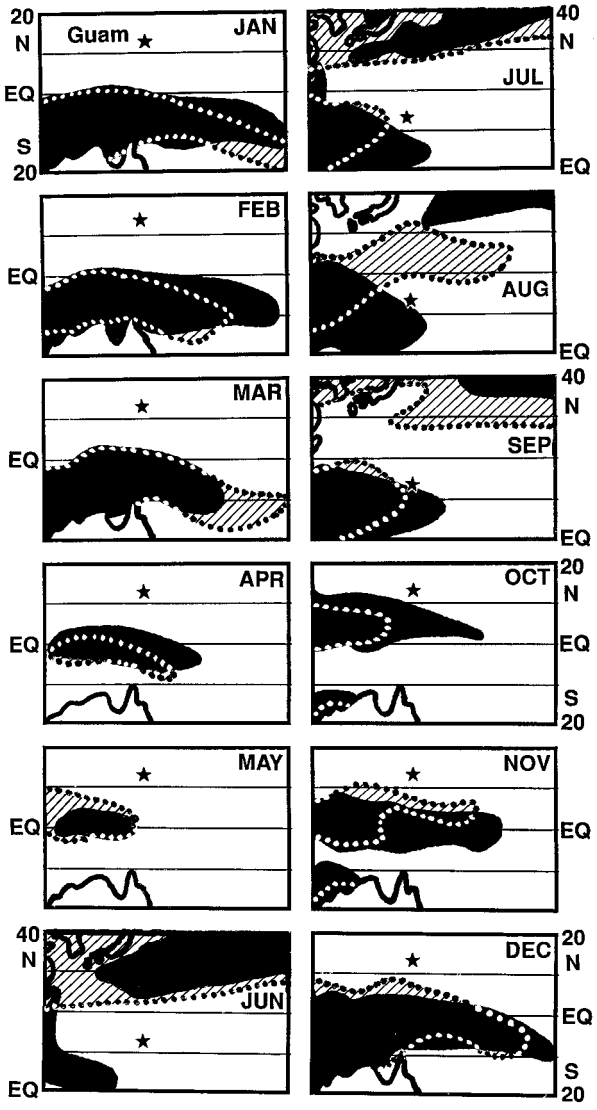

FIG. 3. Comparison between climatological (black regions) and observed (hatched regions) mean monthly winds with a westerly component for the western Pacific in 1996. For Jun, Jul, and Aug the area of coverage is shifted northward to include only the Tropics and subtropics of the western North Pacific. For reference, the star indicates the location of Guam. The outline of Australia appears in the lower left of each panel except for Jun, Jul, and Aug where the Korean peninsula and Japan appear in the upper left. The climatology is adapted from Sadler et al. (1987). The 1996 monthly mean winds were adapted from the CPC (1996).

3) return of near-normal monsoonal westerlies during November and December.

The large number of TUTT cell–related TCs (Sadler 1967, 1976, 1978) is the most distinctive characteristic of the western North Pacific TC distribution during 1996.

A second distinctive characteristic of 1996 was the formation of several TCs at high latitude during a northward displacement of the monsoon trough in August (Fig. 5). The displaced monsoon trough was the site of the development of Kirk (13W), Orson (19W), Piper (20W), and Rick (22W), and TDs 15W, 17W, and 23W. Some of these TCs [e.g., Piper (20W) and Rick (22W)] also formed near TUTT cells.

During November and December of 1996, monsoonal westerlies returned to a near-normal distribution. Two equatorial westerly wind bursts occurred, the first in early November and another in the latter half of December. The November westerly wind burst was associated with the development of the late-season TCs Dale (36W) and Ernie (37W). December's episode of strong equatorial westerly wind was associated with the development of six TCs—three in the Northern Hemisphere [TD 41W, Fern (42W), and Greg (43W)], and three in the Southern Hemisphere [Ophelia (11S), Phil (12P), and Fergus (13P)] (Fig. 6).

The tracks of the TCs that formed in the western North Pacific during 1996 indicate an above-normal number of TCs (10) in the South China Sea (SCS), and an above-normal number (12) of north-oriented tracks [Japan Meteorological Agency (JMA) 1976] (which includes the three ''S'' tracks as a specific type of north-oriented motion). Of the 43 TCs: 9 (21%) were straight movers, 8 (19%) were recurvers, 12 (28%) moved on north-oriented tracks, and 14 (32%) were designated as ''other.'' Of the 12 TCs that moved on north-oriented tracks during 1996, 3 underwent S motion. Ten of the 14 other storms remained in or near the SCS. The three S tracks occurred in association with the high-latitude monsoon trough of August.

An illustration of the TC activity in the entire JTWC area of responsibility during 1996 is provided in Fig. 7. Table 1 lists the significant TCs in the western North Pacific during 1996. Composite best tracks are provided for the periods: 1 January–8 August (Fig. 8a), 9 August–7 October (Fig. 8b), and 8 October–31 December (Fig. 8c).

In summary, 1996 was characterized by more significant TCs than average, more typhoons, and a westward displacement of the mean genesis location. The large-scale oceanic and atmospheric circulation patterns of the tropical Pacific during 1996 indicated the continuation of weak La Niña conditions. Distinctive features of the atmospheric circulation of the western North Pacific during 1996 included more TUTT cell–related TCs, an unusual eastward penetration of the monsoon trough into high latitudes during August, and a return of near-normal monsoonal westerlies during November and December.

b. Summary of monthly activity

1) JANUARY

There were no significant TCs during January.

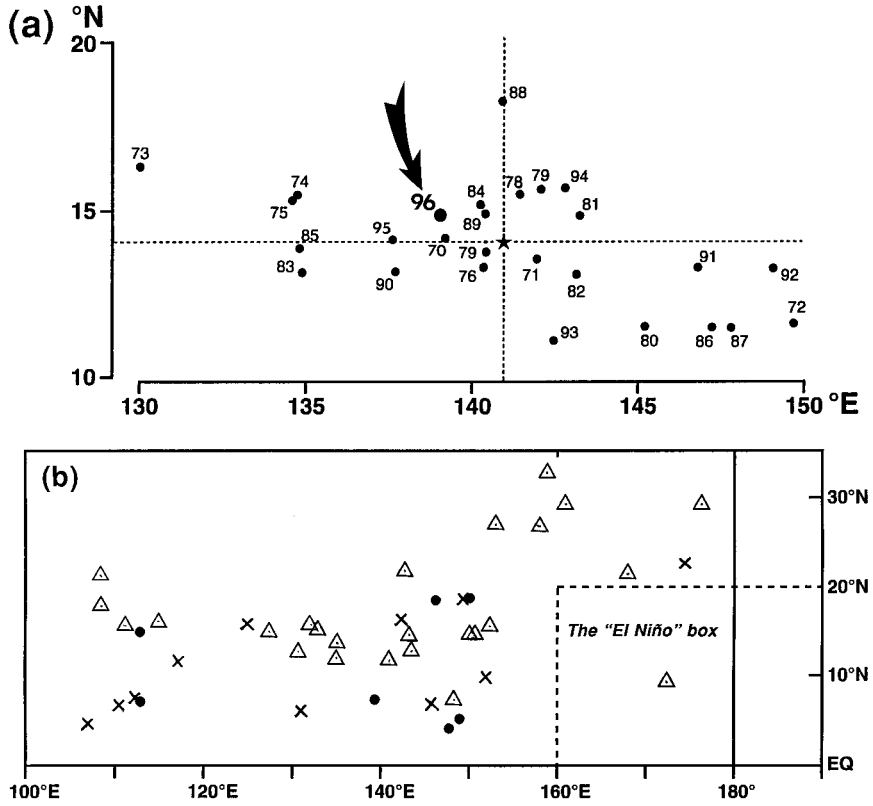

FIG. 4. (a) Mean annual genesis location for the period 1970–96. 1996's location is indicated by the arrow. The star lies at the intersection of the 27-yr average lat and long of genesis. For statistical purposes, genesis is defined as the first 25 kt (13 m s^{-1}) intensity on the best track. (b) Point of formation of significant tropical cyclones in 1996 as indicated by the first intensity of 25 kt on the JTWC best track. The symbols indicate solid dots = 1 Jan–15 Jul; open triangles = 16 Jul–15 Oct; and × = 16 Oct–31 Dec.

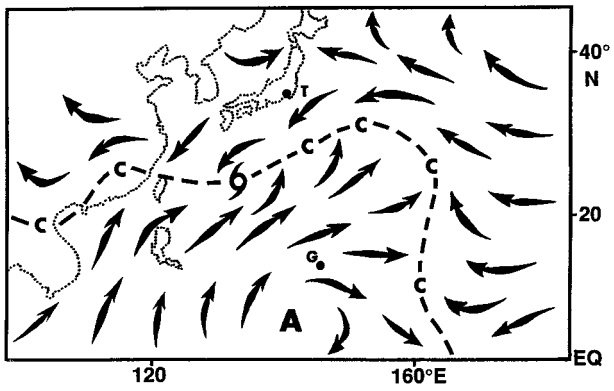

FIG. 5. Schematic illustration of the low-level circulation pattern that dominated the western North Pacific during August 1996. Arrows indicate wind direction, dashed line indicates the axis of the monsoon trough, C indicates low-level circulation centers, A = anticyclone center, G = Guam, and T = Tokyo. A tropical cyclone is shown located along the trough axis.

2) FEBRUARY

For only the fourth time since 1970, a significant TC formed in the western North Pacific during February. Toward the end of the month, Tropical Depression (TD) 01W formed south of Guam. It developed in a temporary near-equatorial trough over the Caroline Islands during a short-lived westerly wind burst. TD 01W moved west-northwest, failed to mature, and on the last day of the month, it moved through the Philippine archipelago just north of Mindanao.

3) MARCH

During the first two days of March, TD 01W completed its passage over the Philippines, entered the SCS, and dissipated. The rest of March in the western North Pacific was relatively inactive, while several TCs originated within the western South Pacific. At the end of March, the western South Pacific became quiet, and a broad, persistent area of deep convection extended westward from Hawaii to central Micronesia. On the last two days of March, the low-latitude tropical disturbance that became Ann (02W) formed southeast of Guam.

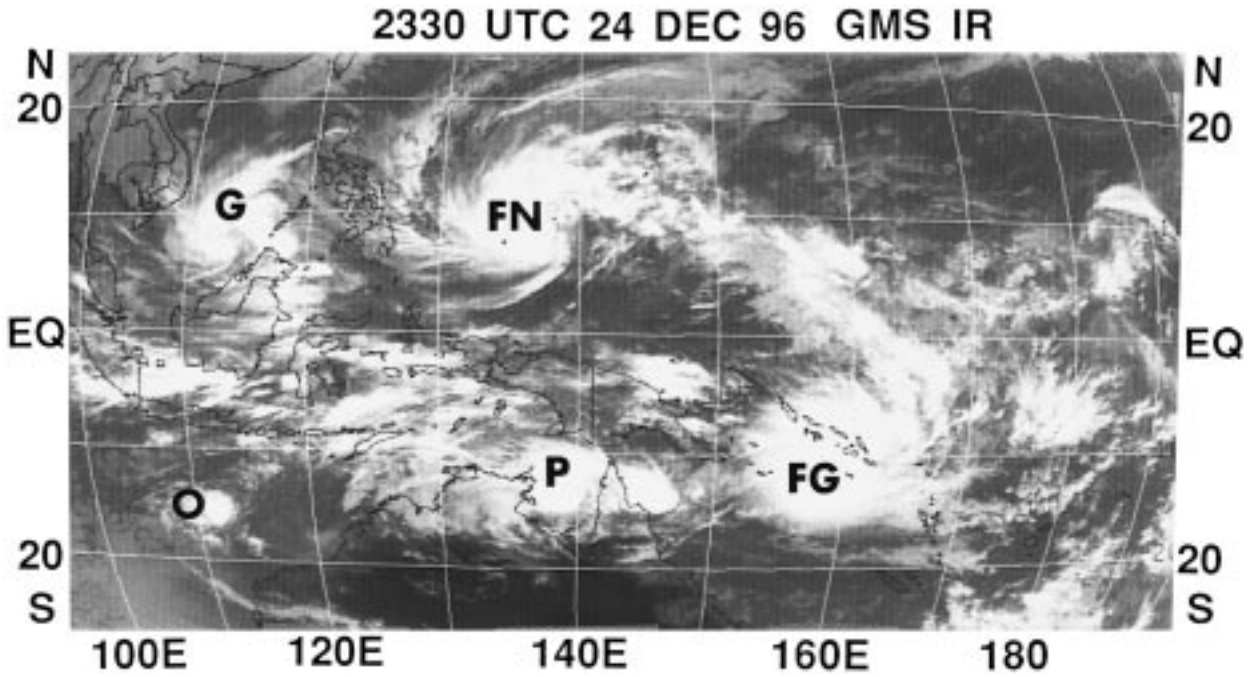

FIG. 6. Five TCs—Greg (G), Fern (FN), Ophelia (O), Phil (P), and Fergus (FG)—lie within twin monsoon troughs. By this time, TD 41W had dissipated near the Malay peninsula.

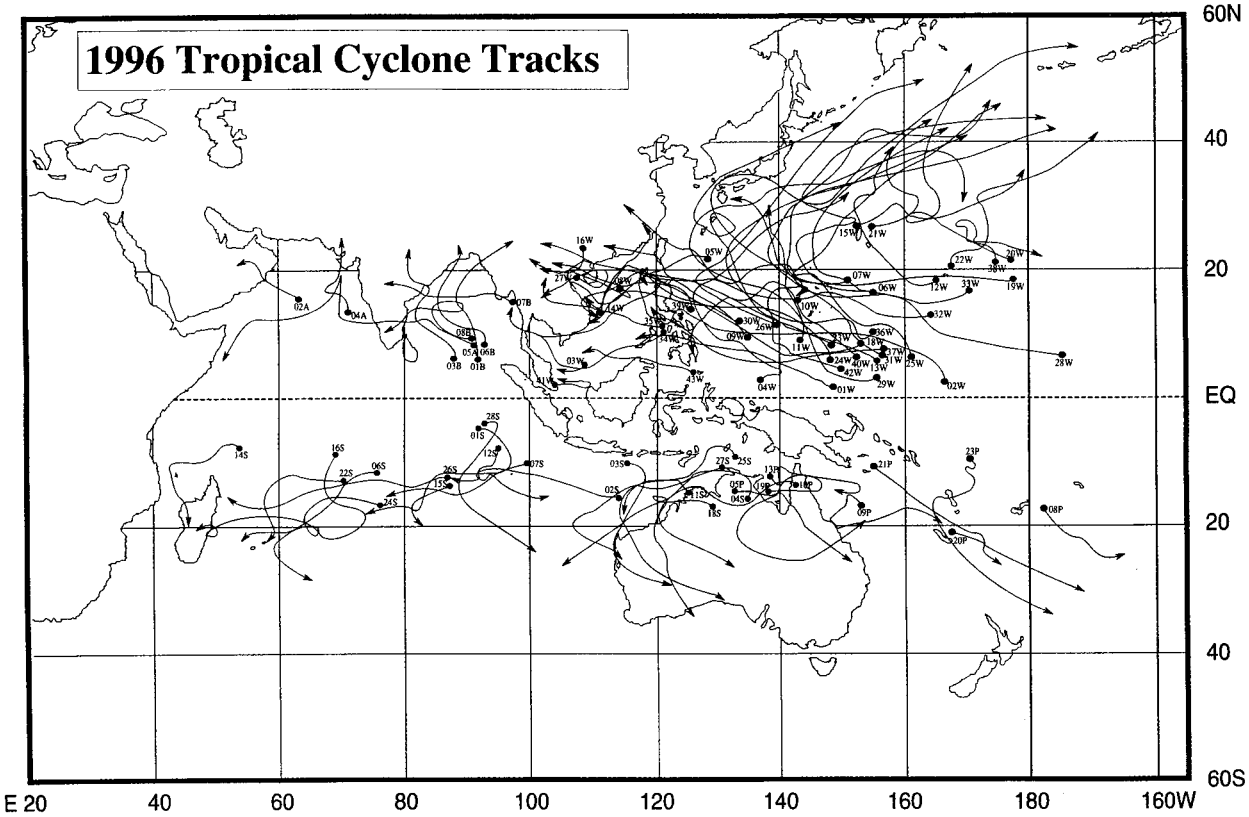

FIG. 7. 1996 JTWC tropical cyclone tracks.

TABLE 1. Western North Pacific 1996 tropical cyclone statistics.

Tropical cyclone number	Name	Class[a]	Dates[b]	Maximum 1-min wind (m s^{-1})	Minimum SLP (mb)
1	(01W)	TD	29 Feb–1 Mar	15	1000
2	Ann	TS	2–9 Apr	21	994
3	(03W)	TD	25–26 Apr	13	1002
4	Bart	TY	9–18 May	64	916
5	Cam	TS	18–24 May	31	980
6	Dan	TY	5–12 Jul	39	967
7	Eve	STY	13–20 Jul	72	898
8	Frankie	TY	21–24 Jul	46	954
9	Gloria	TY	22–27 Jul	46	954
10	Herb	STY	23 Jul–1 Aug	72	898
11	Ian	TS	28–31 Jul	21	994
12	Joy	TY	29 Jul–5 Aug	39	967
13	Kirk	TY	3–16 Aug	49	949
14	Lisa	TS	5–7 Aug	21	994
15	(15W)	TD	12–16 Aug	15	1000
16	Marty	TS	13–14 Aug	26	987
17	(17W)	TS	14–14 Aug	15	1000
18	Niki	TY	18–23 Aug	46	954
19	Orson	TY	21 Aug–3 Sep	59	927
20	Piper	TY	23–26 Aug	33	976
21	(21W)	TD	26–27 Aug	13	1002
22	Rick	TS	28–31 Aug	18	997
23	Sally	STY	5–9 Sep	72	898
24	(24W)[c]	TS	9–14 Sep	23	991
25	Tom	TY	11–20 Sep	39	967
26	Violet	STY	11–23 Sep	67	910
27	Willie	TY	17–23 Sep	33	976
28	Yates	STY	22 Sep–1 Oct	67	910
29	Zane	TY	24 Sep–6 Oct	57	933
30	Abel	TS	11–17 Oct	26	987
31	(31W)	TD	13–17 Oct	13	1002
32	Beth	TY	13–21 Oct	46	954
33	Carlo	TY	21–26 Oct	54	938
34	(34W)	TD	29–30 Oct	15	1000
35	(35W)[c]	TS	2–3 Nov	21	994
36	Dale	STY	4–13 Nov	72	898
37	Ernie	TS	4–17 Nov	26	987
38	(38W)[c]	TS	6–8 Nov	26	987
39	(39W)	TD	8–9 Nov	15	1000
40	(40W)	TD	25 Nov–1 Dec	13	1002
41	(41W)	TD	14–20 Dec	15	1000
42	Fern	TY	21–30 Dec	41	963
43	Greg	TS	24–27 Dec	23	991

[a] TD: tropical depression, wind speed less than 17 m s^{-1}. TS: tropical storm, wind speed 17–32 m s^{-1}. TY: Typhoon, wind speed 33 m s^{-1} or higher. STY: super typhoon, subset of the typhoon category with wind speed greater than 66 m s^{-1}.

[b] Dates begin at 0000 UTC and include only the period of warning.

[c] These TCs were upgraded to tropical storm intensity during postanalysis.

4) APRIL

Two TCs—Tropical Storm (TS) Ann (02W) and TD 03W—were active during April. During the first week of April, Ann became a tropical storm while south of Guam. It moved westward along 10°N and made landfall in the central Philippines, and, on 11 April, dissipated over the eastern SCS. The remainder of April was quiet until the last week, when an area of persistent deep convection northwest of Borneo became TD 03W for a short time span of only 30 h.

5) MAY

By the end of the first week of May, an area of deep convection became organized in the western Caroline Islands as monsoonal low-level westerly winds penetrated eastward to 140°E and south of 5°N. This area of deep convection became Typhoon Bart (04W), the first typhoon of 1996. After a period of rapid intensification, Bart became a very intense typhoon, peaking at 125 kt (64 m s^{-1}) on 14 May. A day later, the intense typhoon recurved to the northeast, and on 19 May it transitioned to an extratropical system near 30°N, 152°E.

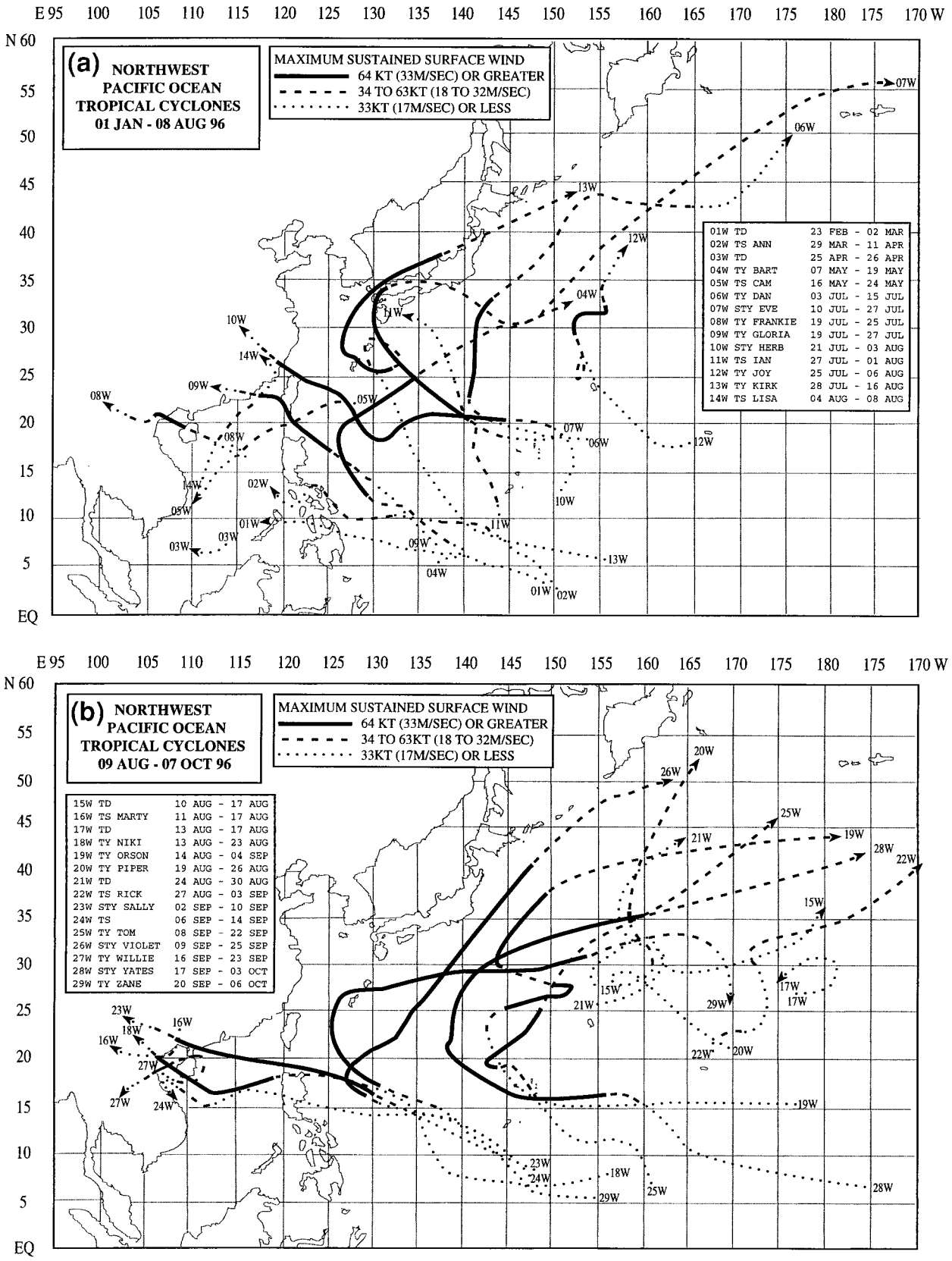

FIG. 8. Composite best tracks for (a) the western North Pacific TCs for the period 1 Jan–8 Aug 1996; (b) 9 Aug–7 Oct 1996; and (c) 8 Oct–31 Dec 1996.

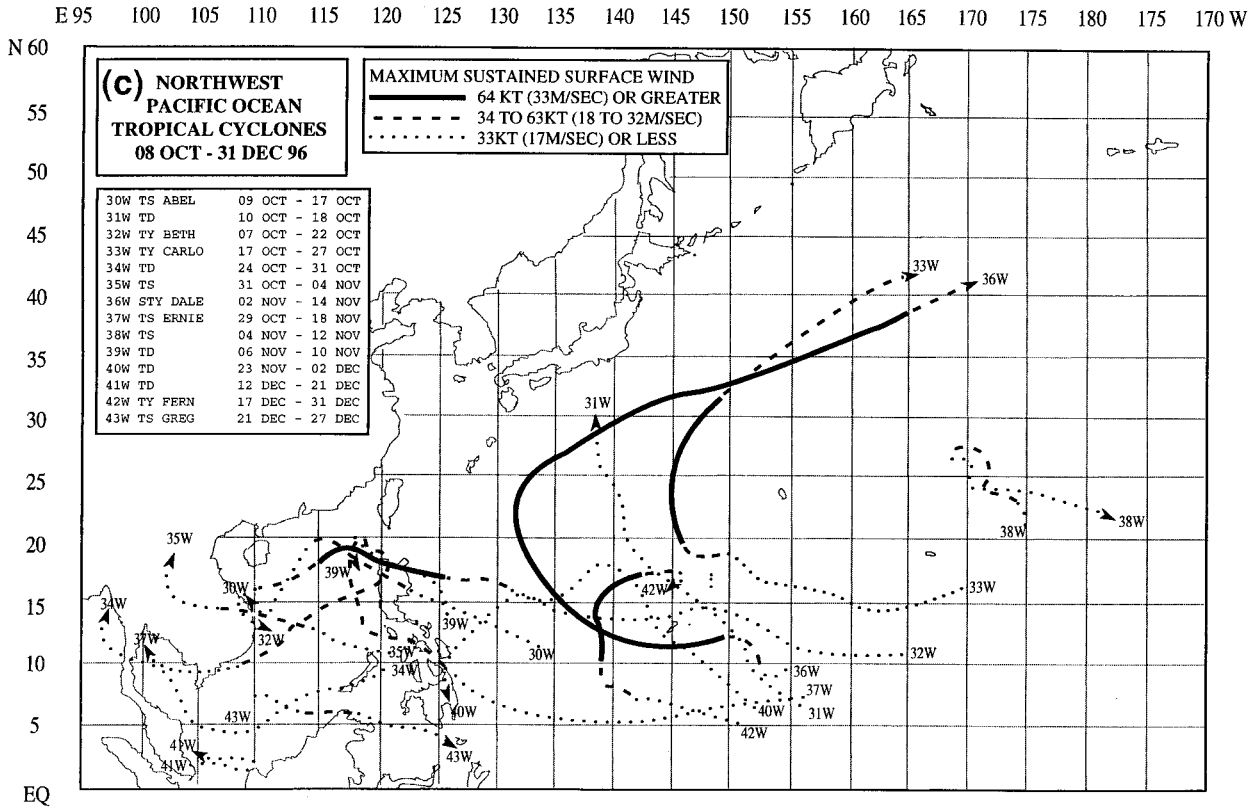

FIG. 8. (*Continued*)

As Bart recurved, southwesterly monsoon flow extended across the SCS east-northeastward toward Bart. Most of the deep convection associated with this flow was located in the SCS as a large cluster of mesoscale convective systems (MCSs) associated with a weak low-level cyclonic circulation and extensive cirrus canopy in anticyclonic outflow aloft. This structure is typical of a monsoon depression. The deep convection consolidated and the system became TS Cam (05W). It passed through the Luzon Strait at peak intensity and then slowly weakened as it drifted eastward into the Philippine Sea and dissipated.

6) JUNE

There were no significant TCs in the western North Pacific during June when deep convection was below normal, low-level winds were anomalously easterly, and upper-level winds were anomalously westerly [Climate Prediction Center (CPC) 1996]. While several tropical disturbances developed during the month, strong vertical wind shear was unfavorable for formation or development. Since 1959, only five other years have had no significant TCs during June.

7) JULY

July produced a total of eight significant TCs. Early in the month, the southwest monsoon had not established itself in the western North Pacific so that large-scale wind anomalies were similar to those of June. Typhoon Dan (06W) and Super Typhoon Eve (07W), formed in association with TUTT cells at relatively high latitude (Dan at 24°N and Eve at 20°N) in low-level easterly flow. On 15 July, Eve underwent a period of explosive deepening (Dunnavan 1981) and reached a peak of 140 kt (72 m s^{-1}) to become the first super typhoon in the western North Pacific during 1996. Eve passed through the northern Ryukyu islands and made landfall in southern Japan.

In the middle of July, the monsoon began to move eastward as the axis of the monsoon trough extended into Micronesia. Extensive deep convection formed an east–west band that extended across from the coast of Southeast Asia to the Marshall Islands. By 21 July, the band consolidated into three distinct cloud clusters, all of which became named TCs: Typhoon Frankie (08W), Typhoon Gloria (09W), and Super Typhoon Herb (10W). Frankie originated from a monsoon depression in the SCS. It became a typhoon in the Gulf of Tonkin and went ashore in Vietnam late on 23 July. While Frankie was developing in the SCS, a monsoon depression in the Philippine Sea became Gloria. Gloria moved northwestward, reached typhoon intensity, and affected Luzon, Taiwan, and eastern China. As Frankie and Gloria moved westward, Herb formed and became the east-

ernmost of three TCs simultaneously active along the monsoon trough. Herb became a super typhoon when east of Taiwan. It was both very intense and large—in fact, the largest TC in the western North Pacific during 1996. Herb made landfall in the southern Ryukyu Islands, Taiwan, and mainland China. On Taiwan, Herb killed 41 people and injured 380 (36 seriously), with 34 others reported missing. Rock slides and flooding were responsible for most of the deaths and injuries. Damage to crops, roads, and power equipment was estimated at U.S. $365 million. It was described as the worst typhoon to hit Taiwan in 30 yr. On a positive note, rainfall from Herb helped to fill reservoirs on Okinawa, averting plans to begin water rationing.

As Herb moved westward toward Taiwan, TS Ian (11W) formed near Guam on the end of the monsoon trough. It moved north-northwestward while embedded in the peripheral southerly flow on the eastern side of Herb (10W). Ian appeared to be adversely affected by Herb's upper-level outflow and did not intensify beyond 40 kt (21 m s^{-1}).

At the end of July, as Herb moved westward, a TUTT cell generated a tropical disturbance in the eastern part of the basin near 20°N, 165°E. The disturbance became Typhoon Joy (12W), but not until 1 August, when it had moved to nearly 30°N. Also by the end of July, a new monsoon trough began to form at low latitudes in Micronesia, replacing the one that had moved with Herb into China. The monsoon depression that became Typhoon Kirk (13W) formed south of Guam in late July, but did not become a named TC until the first week of August.

8) AUGUST

Nine TCs developed during August, and four of the July TCs—Ian (11W), Herb (10W), Joy (12W), and Kirk (13W)—persisted into the early part of the month. On 1 August, Ian dissipated south of Japan. Herb dissipated over eastern China on 3 August. Joy, which had developed near 20°N, 165°E in the last week of July, reached typhoon intensity on 1 August. It moved on a north-oriented track and merged with a frontal cloud band on 6 August. Typhoon Kirk (13W), the last of the July TCs, developed from a monsoon depression at low latitude and did not significantly intensify until it reached 27°N on 5 August. The typhoon moved on a complex north-oriented track, which saw it undergo an unusual clockwise loop before passing directly over Okinawa, where it took a full 12 h for its 70-nm (130 km) diameter eye to pass. Kirk recurved near Okinawa, intensified to its peak of 95 kt (49 m s^{-1}), moved to the northeast, and made landfall in Kyushu on 14 August.

During the period 4–17 August, four relatively weak TCs formed in the western North Pacific. Tropical Storm Lisa (14W) was the first. It originated from a monsoon depression in the SCS. Moving northeastward, the system attained only 40 kt (21 m s^{-1}). Late on 6 August it made landfall in east central China west of the Taiwan Straits. On 12 August, TD 15W developed in the subtropics along the axis of a northward-displaced monsoon trough. This very small depression was influenced by a northward-displaced TUTT and an upper-level cutoff low to the east of Japan. The system dissipated over water on 17 August. TS Marty (16W) originated as a tropical disturbance in the monsoon trough over land in southwestern China. It moved southward into the Gulf of Tonkin and, on 13 August, intensified to a tropical storm. It then turned more to the west, and after a short over-water path it made landfall about 60 nm (110 km) south of Hanoi. Marty destroyed Vietnamese fishing boats in the Gulf of Tonkin where 125 people were reported killed and another 107 missing. TD 17W formed to the east-southeast of TD 15W at the eastern end of the northward-displaced monsoon trough. This TD tracked eastward across the international date line, then doubled back and recrossed the date line to the west. On 17 August after a short life and a short track, TD 17W dissipated over water near 27.5°N, 177°E.

During the middle of August, as TDs 15W and 17W developed along the axis of the higher-latitude monsoon trough, a ridge of high pressure to its south produced easterly low-level winds across the deep Tropics of the western North Pacific. Within these low-latitude easterly winds, several tropical disturbances formed. The tropical disturbance that became Typhoon Niki (18W) can be traced to a small cluster of MCSs, which appeared in the eastern Caroline Islands on 13 August. This disturbance moved westward and developed slowly. It became a tropical storm after it crossed 130°E and before it crossed Luzon. Niki did not become a typhoon until it was in the SCS, where it passed over the southern tip of Hainan Island, crossed the Gulf of Tonkin, and made landfall in northern Vietnam. The tropical disturbance that became Typhoon Orson (19W) developed within a very complex circulation pattern that can best be described as the early stages of the breakdown of the same very high latitude monsoon trough in which Kirk (13W), TD 15W, and TD 17W were located. When the pre-Orson tropical disturbance formed on 15 August, Kirk (13W) was moving eastward over northern Honshu (and becoming extratropical), and TDs 15W and 17W were dissipating at high latitude (30°N) and east of 160°E. For the next four days, the pre-Orson tropical disturbance tracked westward along 15°N. On 19 August, it turned northward and intensified. Orson had a complex history, including two periods of intensification, the formation of a very large eye, and an erratic track.

When Orson became an east-northeastward moving typhoon at 25°N, the monsoon trough was reestablished at a high latitude. The final three TCs of August developed in this monsoon trough at high latitude and were associated with TUTT cells. Typhoon Piper (20W) was very small—easily the smallest typhoon in the western North Pacific during 1996. Developing at a relatively high latitude east of Orson (19W), Piper was located at

the eastern end of the high-latitude reverse-oriented monsoon trough. Piper moved on a north-oriented S-shaped track. On 26 August, Piper accelerated toward the north-northeast and was absorbed into a frontal cloud band east of the Kamchatka peninsula. On 24 August, the weak low-level circulation that became TD 21W developed east of Orson and west of Piper. Sandwiched between these two TCs, TD 21W remained weak in westerly vertical wind shear. After moving on a north-oriented S-shaped track, the system dissipated over water near 42°N, 163°E early on 30 August. TS Rick (22W) formed after Piper and TD 21W moved out of the high-latitude monsoon trough on their north-oriented S-shaped tracks. The tropical disturbance that became Rick was located between Orson (19W) and a well-defined TUTT cell. Rick also became part of the monsoon trough in the eastern end of the trough. It moved on a north-oriented S-shaped track. On 31 August, the system entered the accelerating westerlies north of the subtropical ridge, and by 3 September it dissipated north of 40°N, east of the international date line.

9) SEPTEMBER

September produced seven TCs, including six typhoons (half of which became super typhoons). As the month began, two TCs—Rick and Orson—remained from August. Rick dissipated on 3 September, and Orson became extratropical on 4 September. After the long-lived Orson recurved at the beginning of September, August's unusual monsoon flow pattern gave way to one more in line with climatology: the maximum cloudiness and the axis of the monsoon trough became established from the Philippines east-southeastward into Micronesia. Five TCs—Sally (23W), TS 24W, Tom (25W), Violet (26W), and Willie (27W)—formed in this trough.

Super Typhoon Sally (23W) formed southwest of Guam. It moved on a relatively steady west-northwest straight-moving track. It became a super typhoon while moving through the Luzon Strait, and later, though weaker, it made landfall in southwestern China where it was reported to have killed 114 people. The city of Zhanjiang on the east coast of the Luichow peninsula was one of the hardest hit areas of southern China—79 people were reported killed there. Almost all trees in this city and its suburbs were reported to have been uprooted by high winds. Economic losses were described as the worst since 1954. Combined losses in the cities of Zhanjiang and Maoming were estimated at U.S. $1.5 billion. TS 24W (unnamed) began as a tropical disturbance located near Guam. By the morning of 9 September it became a large monsoon depression in the Philippine Sea. The system moved westward, crossed Luzon, and entered the SCS. On 14 September, it moved into the Gulf of Tonkin where it dissipated. The upgrade to a tropical storm was based upon a postanalysis of synoptic data, which indicated that the sustained winds reached a peak of 45 kt (23 m s^{-1}) when the TC was in the SCS.

The next two September TCs—Typhoon Tom (25W) and Super Typhoon Violet (26W)—moved in tandem along adjacent recurving tracks. Although both TCs had large circulations, their separation distance (2050 km) was too great for binary interaction. When Tom reached its peak intensity of 75 kt (39 m s^{-1}) on 16 September, it had an unusual ''pinhole'' eye in a small central cloud mass surrounded by extensive peripheral rainbands within a large outer wind circulation. By contrast, Violet was as large as Tom, but with a much different structure: Violet's eye began small, but then expanded to a 75 n mi (140 km) diameter. Violet killed 7 people and injured 44 in southeastern Japan.

TS Willie (27W) developed in the Gulf of Tonkin. Willie was a small TC and was part of a three-TC outbreak along the monsoon trough, with the larger TCs Tom and Violet to its northeast. Never more than 90 n mi (170 km) from shore, Willie circumnavigated Hainan Island in a counterclockwise loop.

The tendency of the monsoon trough of the western North Pacific to form and then migrate northward lends itself to a natural segregation of TCs into ''families'' associated with the same monsoon trough. The five-TC sequence of early September—Sally, TS 24W, Tom, Violet, and Willie—had this common origin. By late September, the monsoon trough moved northward, became reverse-oriented, and migrated to higher latitude as TCs Tom and Violet carried it with them out of the Tropics. As this monsoon trough left the Tropics, a new one formed at low latitudes. It was the site of development for the next two TCs: Super Typhoon Yates (28W) and Zane (29W). Like Tom and Violet before them, Yates and Zane developed at approximately the same time in the same trough, and recurved simultaneously along similarly shaped adjacent tracks. Yates and Zane had motion characteristic of semidirect and indirect TC interaction (Carr and Elsberry 1994).

10) OCTOBER

At the beginning of October, Yates and Zane recurved and moved into the midlatitudes. For about one week, during this time, the low latitudes became relatively free of deep convection, and there was a break in TC activity. By the end of the first week of October, deep convection began to increase in low latitudes, and winds throughout most of Micronesia became light and variable as yet another monsoon trough became established. The first three TCs of October—Abel, TD 31W, and Typhoon Beth—developed in the low-latitude cloud band over the span of three days. TS Abel (30W) originated from a monsoon depression in the Philippine Sea, crossed Luzon, and became a tropical storm in the SCS. Forced to move southwestward by the northeast monsoon, it dissipated over water as it approached the coast of southern Vietnam. Moving toward the northwest, TD 31W

exhibited a sheared cloud pattern throughout its life. On 17 October, the deep convection associated with TD 31W decreased and became sheared well to the east of the low-level circulation center as the system dissipated over water. The tropical disturbance that became Typhoon Beth (32W) was first detected in the eastern Caroline Islands. For a week, it developed very slowly. As it passed over Guam, it produced an unusual event (in the maritime Tropics): a spectacular display of cloud-to-ground lightning. On 16 October, Beth became a typhoon in the Philippine Sea and later passed over Luzon where it caused at least three deaths. In the hardest-hit province of Cagayan, Beth damaged municipal buildings, crops, and eroded roads. Encountering the northeast monsoon in the SCS, it turned to the southwest, weakened, and made landfall in central Vietnam.

While Abel (in the South China Sea), TD 31W (east-southeast of Okinawa), and Beth (32W) (near the coast of Luzon) were active in the western part of the western North Pacific, elsewhere in the Tropics the amount of deep convection was below normal and the low-level wind was predominantly from the east. The only area of deep convection considered to have a potential for TC formation was associated with a TUTT cell centered near 17°N, 168°E. Typhoon Carlo (33W) formed in association with this TUTT cell. After recurving, Carlo accelerated to 30 kt (55 km h^{-1}) and was absorbed into the frontal cloud band of an intense extratropical low on 27 October.

In late October, TC development shifted to the SCS. On 25 October, TD 34W developed just west of the Visayan Islands of the Philippines. The small weak TC moved to the west-southwest and, as it approached the Malay peninsula, turned toward the northwest. TD 34W passed through the Gulf of Thailand, moved across the Isthmus of Kra into the Bay of Bengal, and then dissipated over southern Myanmar on 31 October. On the last day of the month, the monsoon depression that became TS 35W formed over the Philippines at nearly the same location where TD 34W originated. It did not become a tropical storm until early November. TS 35W was a larger system than TD 34W as a monsoon depression. It moved across the SCS and made landfall in central Vietnam. The upgrade to TS intensity was based upon postanalysis of ship reports and satellite imagery.

11) NOVEMBER

From late October through the first day of November, the Tropics of the western North Pacific (except the SCS) were dominated by low-level easterly wind and upper-level westerly wind. Deep convection was disorganized and widely scattered. On 2 November (the same day that TS 35W became a tropical storm in the SCS), the amount of deep convection in the low-latitudes of the western North Pacific began to increase as pressures fell throughout Micronesia during the onset of a near-equatorial trough along 5°N. On 3 November, the deep convection consolidated into two distinct clusters: one near 8°N, 150°E that became Super Typhoon Dale (36W), and the other near 7°N, 138°E that became TS Ernie (37W). Super Typhoon Dale (36W) was a large and very intense typhoon with an extensive area of monsoon gales to its south and southwest. The equatorial westerly wind burst that accompanied Dale's formation was associated with extremely low sea level pressure reports along the equator. Passing 110 n mi to the south of Guam late on 7 November, the typhoon generated phenomenal seas and surf that pounded the island for three days. Dale recurved, and on 14 November, it transitioned into an intense extratropical cyclone at 40°N. TS Ernie (37W) originated from a westward-moving tropical disturbance first noted on 29 October in the eastern Caroline Islands. For several days the pre-Ernie tropical disturbance moved westward before showing signs of development on 3 November. The system became a tropical storm only a few hours before making landfall in northern Mindanao. Ernie crossed the Philippines and entered the SCS where it reached its peak intensity of 50 kt (26 m s^{-1}). While undergoing a clockwise loop west of Luzon, the system merged with TD 39W, and later moved toward the west-southwest in association with a surge in the northeast monsoon to its north. On 18 November, the weakened TC dissipated in the Gulf of Thailand.

The rest of the November TCs were weak. TS 38W (unnamed) developed from an unusually late-in-the-year TUTT cell located to the northeast of Dale. The system moved erratically for nearly eight days (4–12 November). It dissipated on 12 November near 22°N, 179°W, approximately 180 nm (335 km) east of where it formed. Late on 6 November, TD 39W formed between Dale and Ernie as they were moving toward the west. Located within 200 nm (370 km) of one another, TD 39W and Ernie underwent a binary interaction and merged when, on 10 November, the weakened TD 39W was absorbed into Ernie.

After Dale recurved, and Ernie and TD 39W moved into the SCS, the western North Pacific experienced a break in TC activity associated with rising sea level pressure and light winds at low latitude. After a week-long lull, an extensive area of deep convection formed in Micronesia, although low-latitude sea level pressure remained high. On 23 November, the deep convection evolved into a large monsoon depression centered near Chuuk. Moving northwestward toward Guam, the depression became TD 40W. It moved to 18°N, where it ran into a region of enhanced northeasterly low-level flow. The system then became sheared, drifted toward the southwest, and dissipated over Mindanao on 2 December.

12) DECEMBER

After the demise of TD 40W over the southern Philippines on 2 December, activity subsided in the western

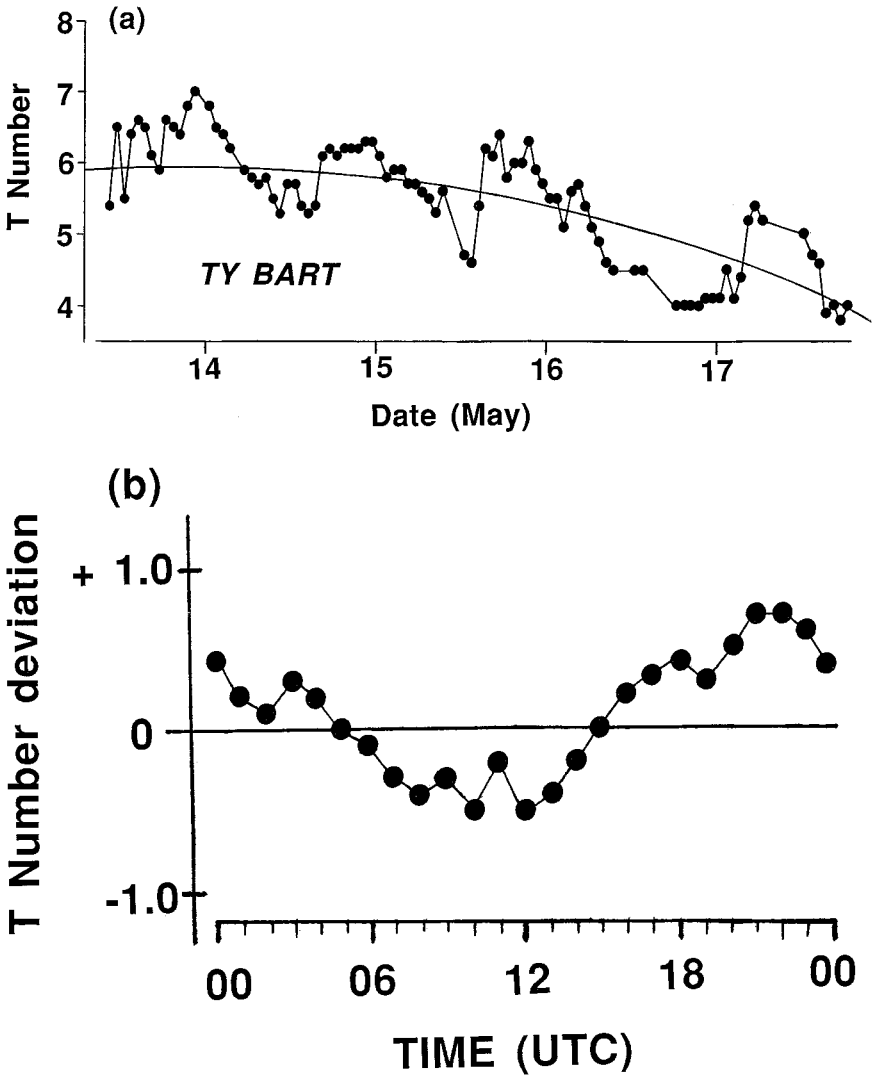

FIG. 9. (a) Bart's DD time series for the period 1030 UTC 13 May–1530 UTC 17 May. (b) The diurnal cycle of Bart's DD time series as obtained by averaging the DD numbers at each hour during the period 1030 UTC 13 May–0930 UTC 16 May 1996.

North Pacific until mid-December when deep convection associated with a developing equatorial westerly wind burst began to increase across Indonesia and eastward along the equator to near 160°E. Low-latitude low-level westerly winds gradually increased to 40 kt (21 m s^{-1}) with gusts to 50 kt (26 m s^{-1}) extending from Indonesia to 155°E and bounded by the axes of twin low-latitude monsoon troughs. A total of six TCs—three in the Northern Hemisphere [TD 41W, Fern (42W), and Greg (43W)], and three in the Southern Hemisphere [Ophelia (11S), Phil (12P), and Fergus (13P)]—formed along the respective monsoon trough axis. On 13 December, synoptic data indicated that a weak low-level circulation center was located at low latitude east of the Malay peninsula associated with deep convection in the region. The low-level circulation center moved eastward and became TD 41W on 14 December. The system moved eastward toward Borneo, then on 16 December, as it neared the northwest coast of Borneo, it doubled back and moved westward. Continuing westward, it dissipated on 21 December approximately 90 nm (165 km) from where it formed.

Typhoon Fern (42W) formed southeast of Guam at low latitude and had a Southern Hemisphere twin, Fergus (13P97). Fern moved west-northwestward, and turned to the north on Christmas Day when it was west of Yap. Fern attained its maximum intensity of 80 kt (41 m s^{-1}) on 26 December. The weakening typhoon dissipated 150 nm (280 km) northeast of Saipan on the last day of the month.

The final western North Pacific TC of 1996, TS Greg (43W), developed in the South China Sea midway between Vietnam and Borneo. It moved eastward at low latitude throughout its life, apparently steered by the

strong westerly winds associated with an intense westerly wind burst to its south. The TC reached its peak intensity of 45 kt (23 m s^{-1}) on Christmas Day. On the following morning it made landfall in an unusual location: the northern tip of Borneo in the east Malaysian State of Sabah near the city of Kota Kinabalu. In Sabah, at least 124 people were reported killed and 100 others were missing primarily due to flooding from torrential rains. In Kota Kinabalu, high wind scattered billboards and other debris, and broke windows in the 30-story government building. Greg continued its unusual eastward motion and dissipated on 27 December at 3°N in the eastern Celebes Sea.

c. Noteworthy tropical cyclones

This section highlights nine TCs that had unusual structures or histories.

1) TYPHOON BART (04W)

Bart had an unusually pronounced diurnal cycle in its satellite-estimated intensity that was best illustrated in its digital Dvorak (DD) time series. The DD algorithm—developed by R. Zehr (1997, personal communication) and programmed by G. Schaeffer (1997, personal communication)—adapts the rules of the Dvorak satellite TC intensity estimation techniques as subjectively applied to enhanced infrared imagery (Dvorak 1984) in order to arrive at an objective *T* number, or ''digital Dvorak'' (DD) number. Infrared imagery is available hourly from the Japanese Geostationary Meteorological Satellite, and hourly DD numbers were calculated for all of the typhoons of 1996. The DD numbers are experimental. In some cases, the DD numbers differ substantially from the warning intensity and also from the subjectively determined *T* numbers. The output of the DD algorithm often undergoes rapid and large fluctuations. The JTWC relies almost exclusively on satellite imagery to diagnose TC intensity, and the DD numbers may lead to modifications in the current subjective methods of estimating TC intensity from satellite imagery.

In Dvorak's 1975 and 1984 papers, he advises that the intensity estimation from satellite imagery be made at 24-h intervals in order to remove any possible diurnal cycles that might bias the estimate of the TC intensification rate. Diurnal variations of convection reported to occur in TCs are similar to those reported to occur over the maritime Tropics in general: a peak in the amount of very cold cloud tops during the early morning hours with warmer cloud-top temperatures during the afternoon (Dvorak 1984; Zehr 1992). Observations by Black and collaborators (e.g., Black 1983; Black et al. 1986; Black and Marks 1987) show that major cold convective eruptions in TCs tend to be initiated in the early morning.

Bart is one of only a few cases in which a strong diurnal cycle appears in the time series of its DD numbers (Fig. 9a). Although the DD number is based upon both the cloud-top temperature of the eyewall cloud and the temperature within the eye, the strong diurnal cycle in Bart's DD time series (Fig. 9b) is certainly linked to a diurnal cycle of the eyewall cloud-top temperatures. The DD time series of Bart has an unusually strong diurnal cycle when compared with those of other typhoons of 1996 and with those typhoons of 1995 for which the DD time series was compiled. Consistent with Dvorak's rules, Bart's warning and best-track intensities do not contain the large diurnal fluctuations that appear in its DD time series.

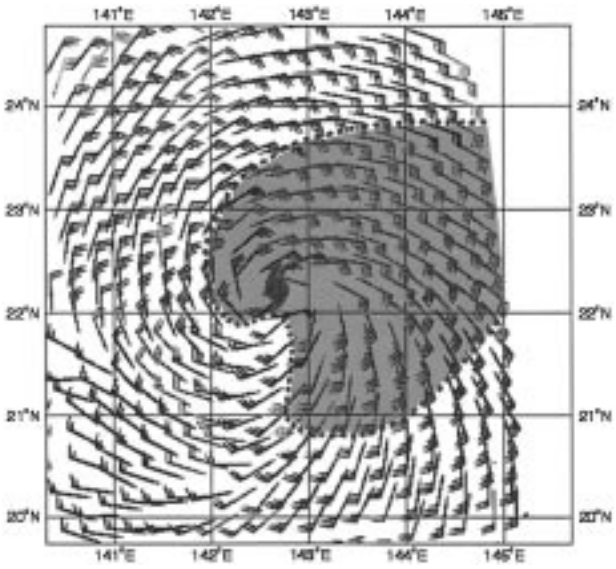

FIG. 10. Scatterometer-derived wind speeds in a swath that passed over Dan (1304 UTC 7 July *ERS-2* scatterometer-derived marine surface wind speeds). Gale area is shaded. This product was used in real time to expand the area of gales on the TC warning. (Note: 30-kt *ERS-2* winds indicate 1-min sustained minimal gales.)

2) TYPHOON DAN (06W)

A large underestimate of Dan's distribution of gales, and problems with the intensity diagnosis during its extratropical transition, prompted Dan's inclusion in this section.

On the warning valid at 1800 UTC 17 July, Dan's radius of 35 kt (18 m s^{-1}) wind was nearly doubled from its value on the warning valid at 1200 UTC 7 July. This large change in the wind radius was based upon scatterometer data from the European Remote Sensing Satellite-2 (*ERS-2*) (Fig. 10). The JTWC has access to scatterometer wind data and has used it to help determine the position, intensity, and wind distribution of TCs. In three years of using scatterometer data, it has become a valuable diagnostic tool, especially in the determination of TC outer wind distribution.

Another problem the JTWC has had for many years

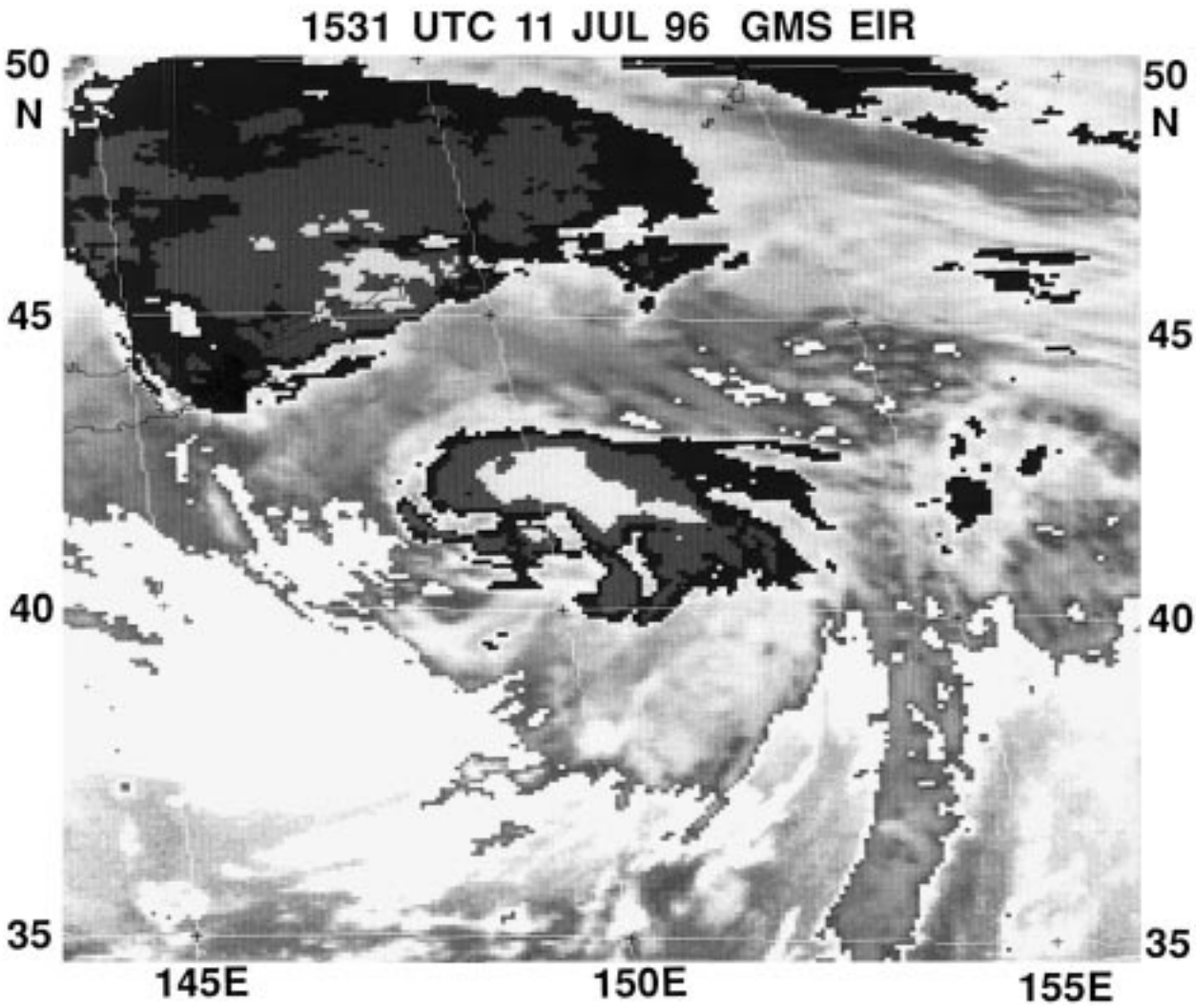

FIG. 11. Dan begins its extratropical transition. Satellite intensity estimates as low as 35 kt (18 m s^{-1}) at this time were far lower than the ship reports of 60 kt (31 m s^{-1}), which were used to support the best-track intensity.

is diagnosing the intensity of TCs as they undergo extratropical transition. In general, the application of Dvorak's techniques to these systems has resulted in intensity estimates that are significantly lower than what is reported by ships or land stations. An extreme example of this problem occurred during the approach of Seth (1994) to Korea, which is highlighted in Seth's summary in JTWC's 1994 Annual Tropical Cyclone Report (JTWC 1994). Dan provided another good example of this problem: as it was becoming extratropical (Fig. 11), the satellite intensity estimates fell to values that were later proven to be far too low when compared to ship reports. Attempts to apply Hebert and Poteat's (1975) techniques for estimating the intensity of subtropical cyclones to these systems were not successful.

To address the problem of underestimating the intensity of TCs as they undergo extratropical transition, satellite forecasters at the JTWC in conjunction with Office of Naval Research–supported researchers at the University of Guam devised a technique (Miller and Lander 1997) for estimating the intensity of TCs undergoing extratropical transition. The technique yields XT (for extratropical transition) numbers that equate to wind speeds identical to Dvorak's *T* numbers of the same magnitude. The technique also defines the completion of extratropical transition. On the few independent cases for which it was applied during 1996, the technique appears to have worked well. Though now used operationally at the JTWC, the technique may be refined as more cases are examined.

3) SUPER TYPHOON HERB (10W)

Herb was the largest typhoon in the western North Pacific during 1996. It had an unusual history with three intensity peaks contained in its DD time series. As it

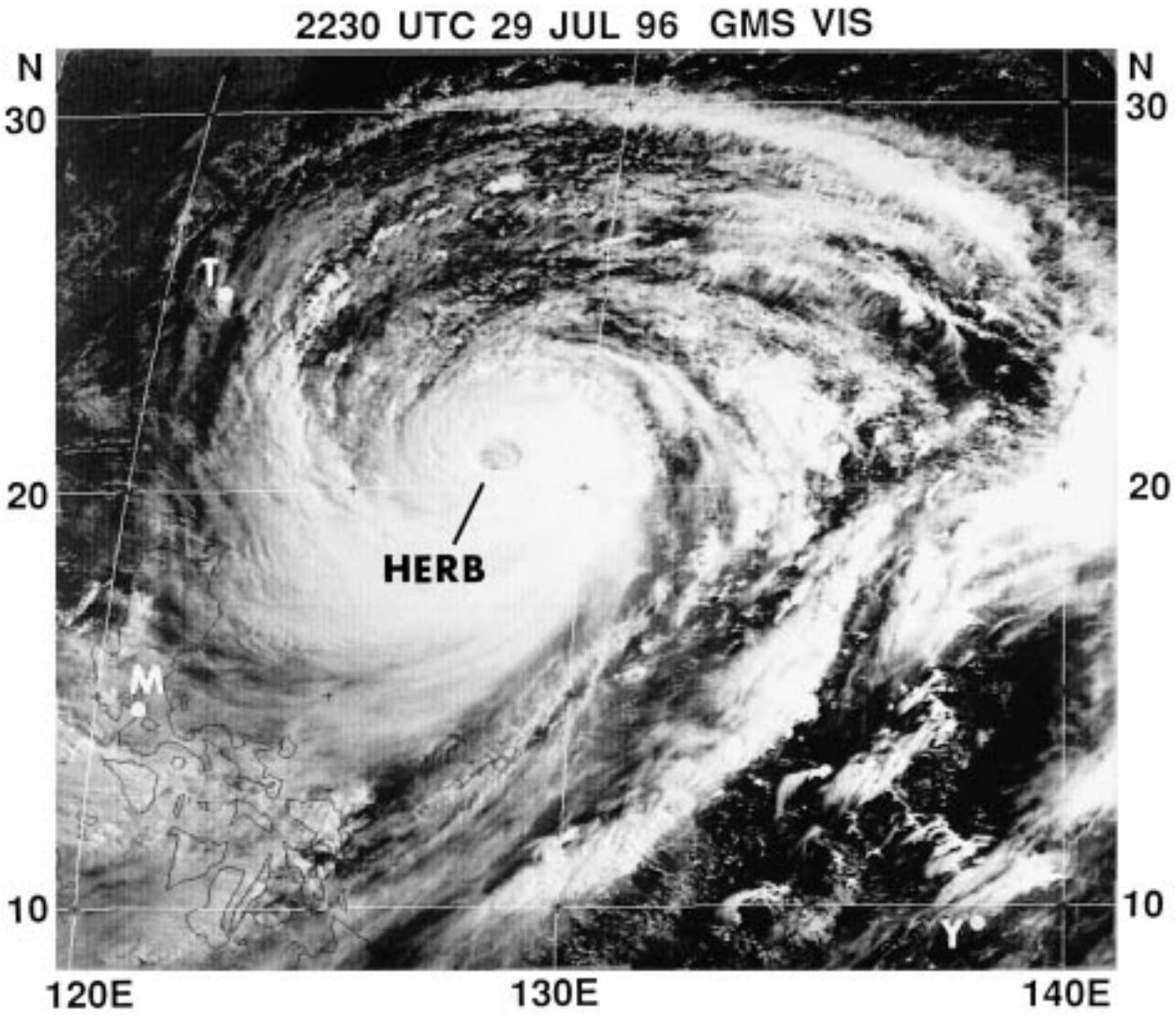

FIG. 12. Cyclonically curved low-level cloud lines extending hundreds of kilometers from Herb's core and primary rainband indicate the very large size of Herb's peripheral circulation: T = Taipei; M = Manila.

approached Taiwan, good radar coverage was obtained from a newly installed NEXRAD. Herb passed over Taiwan's NEXRAD site, severely damaging the radar, but not before a unique dataset was collected for this very intense TC.

By some measures of TC size, Herb (Fig. 12) was the largest TC of 1996. Using the mean radius to the outermost closed isobar (ROCI) as a measure of Herb's size, the system surpassed the threshold of the ''very large'' size category used by the JTWC. At its largest, the mean ROCI of Herb was about 8.5° of a great-circle arc.

Tropical cyclone size is a very difficult parameter to measure objectively. Merrill (1984) classified a tropical cyclone as ''small'' if the mean ROCI was three degrees (180 nm, 335 km), or smaller; as ''medium'' if the mean ROCI was between three and five degrees (180–300 nm; 335–555 km), and as ''large'' if the mean ROCI was greater than five degrees (greater than 300 nm, 555 km). The Japan Meteorological Agency recognizes two additional size categories—''very small'' and ''ultra-large''—that mesh neatly with Merrill's scheme. The definitions of size used by JTWC have been adapted by a synthesis of Japan's size categories with those of Merrill.

The time series of the DD numbers obtained for Herb (Fig. 13) indicate three maxima: one at approximately 0000 UTC 27 July, a second at approximately 1800 UTC 28 July, and a third on 30 July. Dvorak's techniques require that the warning intensity should match the *T* number when the *T* number is rising, and then remain higher than the *T* number when the *T* number falls. For the most part, this is true of a comparison of Herb's DD time series with its final best-track intensities (Fig. 13).

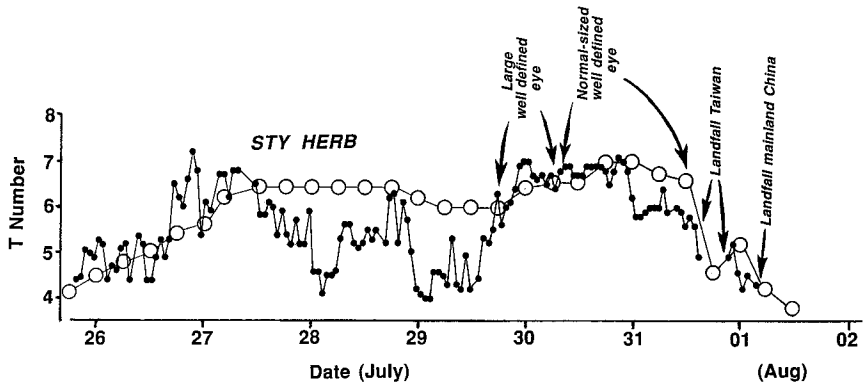

FIG. 13. The time series of Herb's hourly DD numbers (small dark circles) with the final best-track intensity (large open circles) superimposed.

Note that the DD time series contains some rather large fluctuations that do not appear in the final best-track intensity time series. It is not known to what extent the fluctuations in the DD time series may represent actual short-term changes in the intensity of TCs.

As Herb made landfall in Taiwan, a NEXRAD on the northeast coast—directly in Herb's path—detected eyewall mesocyclonic vortices (EMVs). EMVs were first detected and documented in airborne Doppler radar data by Marks and Houze (1984) and also with aircraft inertial navigation equipment as noted by Black and Marks (1991). Stewart and Lyons (1996) identified EMVs with the Guam NEXRAD in association with the passage of Ed (1993) over Guam. Until the implementation of the NEXRAD radar network in the United States during the early 1990s, only chance encounters with EMVs have occurred during reconnaissance aircraft penetrations. However, now that Doppler velocity data are available, strong mesocyclones associated with TC outer convective bands and eyewall convection are frequently detected.

Stewart et al. (1997) used NEXRAD data to show that mesocyclonic vortices in the wall clouds of TC eyes may be a mechanism for TC intensification and for extreme wind bursts in TCs as noted with Hurricane Andrew damage (Wakimoto and Black 1993). In three cases (including Herb), a TC rapidly intensified when several vertically deep EMVs formed prior to the occurrence of rapid intensification and persisted for several hours while rapid deepening occurred. Comments from Stewart et al. (1997) include the following.

> Approximately three hours prior to landfall in Taiwan, satellite imagery indicated Herb had weakened . . . In contrast, the [Taiwan NEXRAD] indicated that Herb was actually intensifying . . . As early as 310656Z July, [the NEXRAD] indicated intense EM[V]s had begun to develop and this trend continued until the last available data at 311350Z [when the data record ended because of damage to the radar by high wind] . . . Although the [Taiwan NEXRAD] detected several EM[V]s (as many as 6 EM[V]s occurred simultaneously in the eyewall), one particular EM[V] became quite intense and persisted for more than 1.5 hours just prior to Herb's landfall . . . This particular EM[V] peaked at 311314Z with a rotational shear of 0.075/sec which is more than *triple* the [NEXRAD] criteria for a Tornadic Vortex Signature . . ..

Based on observations of EMVs in TCs (including Herb), Stewart et al. (1997) conclude that the EMVs appear to have a positive feedback on TC intensification.

4) TYPHOON KIRK (13W)

Kirk possessed a very large eye as it passed over Okinawa. This unusual feature was observed in detail by the U.S. Air Force's NEXRAD on Okinawa.

In Dvorak's analysis techniques (Dvorak 1975, 1984), the eye of a TC is considered small if its satellite-observed diameter is less than 30 n mi (55 km), average if between 30 and 45 n mi (55 km and 85 km), and large if greater than 45 n mi (85 km). Kirk's satellite-observed eye diameter was in excess of 70 n mi (150 km) for most of 12 August (the day it passed over Okinawa) (Fig. 14). This very large eye required 12 h to pass across the island. Kirk was one of three TCs of 1996—the others were Orson (19W) and Violet (26W)—that possessed, at some time during their evolution, an eye with an exceptionally large diameter (on the order of 75 n mi). Eye diameters on the order of 75 n mi, or greater, are not common. None were observed in 1995.

In a survey of past Annual Tropical Cyclone Reports, the largest eye diameter ever reported was that of Typhoon Carmen (JTWC 1960). By coincidence, Carmen, like Kirk, passed directly over Okinawa. Carmen's eye diameter, as measured by the weather radar at Kadena, was 200 n mi (370 km). Comments in the 1960 Annual Typhoon Report include the following.

> Another feature quite unusual about this typhoon was the diameter of its eye. Reconnaissance aircraft frequently reported eye diameters of 100 [n] mi, using as the basis of measurement, surface winds and pressure gradient.

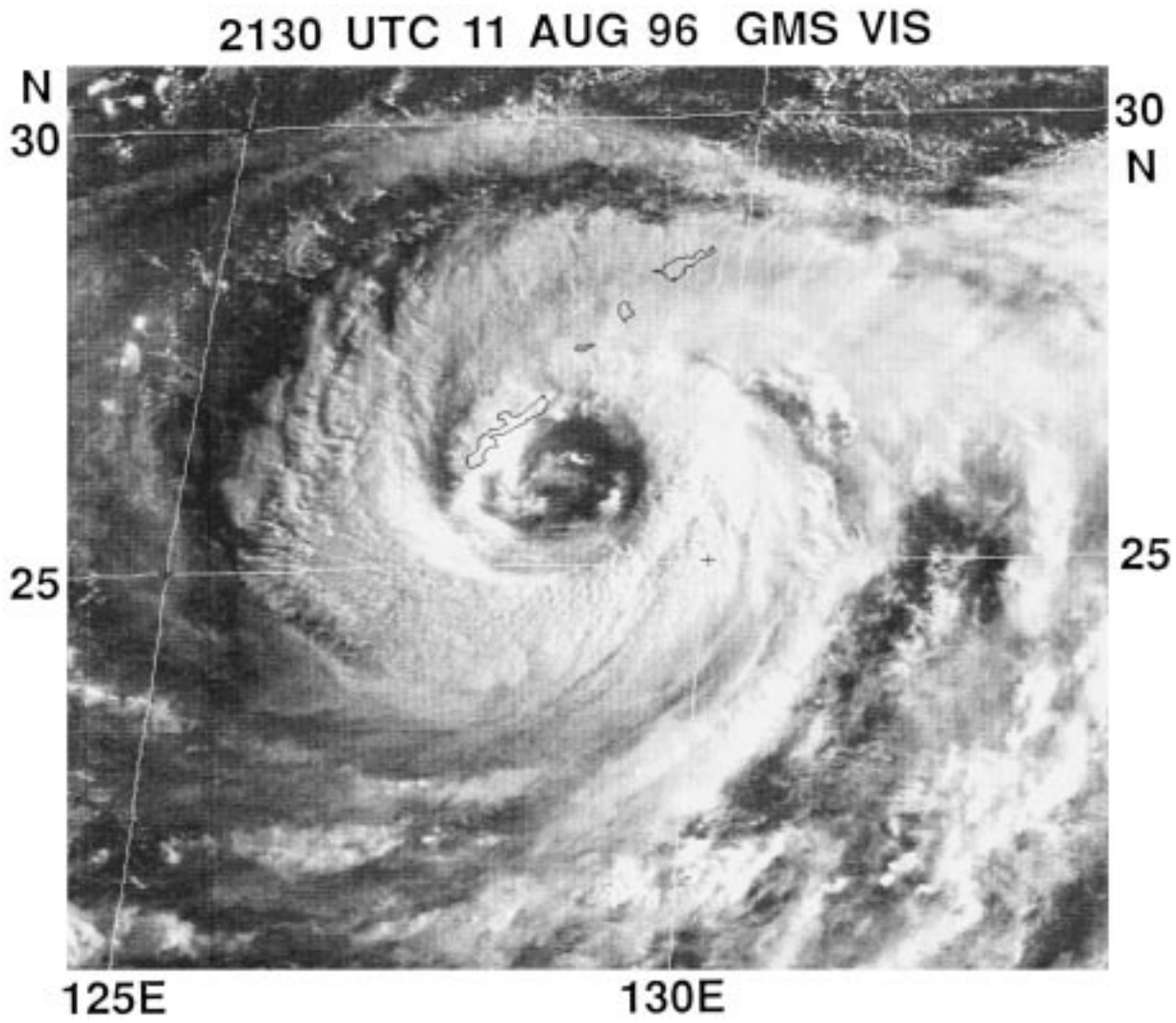

FIG. 14. Typhoon Kirk's very large eye as seen in the low sun angle of early morning just prior to moving over the island of Okinawa.

> However, with respect to wall clouds surrounding the eye, radar photographs taken from the CPS-9 at Kadena AB show quite clearly that on 20 August, the eye had a diameter of approximately 200 [n] mi . . . The eye diameter of Carmen was probably one of the largest ever reported . . ..

Kirk, like Carmen, was also viewed by a radar at Kadena: this time a new NEXRAD. One of only four NEXRAD radar units to be installed by the U.S. military in the western North Pacific (the others are on Guam and in Korea), the NEXRAD installed on Okinawa affords an excellent opportunity to gather data on the TCs, which frequently pass near or over this island. When Kirk passed directly over Okinawa, it was continuously under surveillance by NEXRAD. During 12 August, as Kirk passed over the radar site from east to west, the eye diameter was reported to have been consistently on the order of 60 n mi (110 km) (Fig. 15). This is about 10–15 n mi less than the eye diameters as derived from satellite imagery during this time. It is common that the eye diameter as observed from satellite is larger than the radar-observed eye diameter due to the general outward sloping with height of the eyewall cloud.

Another fascinating aspect of the radar coverage occurred when the radar was exactly in the center of the eye: the Doppler velocity product indicated almost zero velocity along all radials. This is certainly what might be expected, but it may be the first time that it has actually been seen. Another feature of the velocity product at this time was a slight asymmetry in the radial velocity, which was mostly light inbound to the east-southeast and light outbound toward the west-northwest, indicative of the motion of the typhoon.

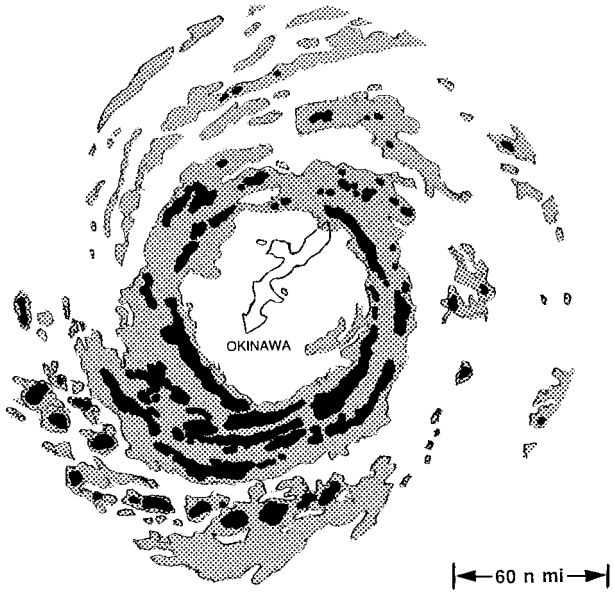

FIG. 15. A radar depiction of Kirk while it was over Okinawa. Shaded regions indicate reflectivity values of at least 30 dBZ, and the black regions indicate reflectivity values of at least 40 dBZ. (Depiction based upon the 0611 UTC 12 Aug NEXRAD composite reflectivity product.)

5) TYPHOON PIPER (20W)

Like most TCs that form at high latitude in association with TUTT cells, Piper was a very small TC—the smallest in the western North Pacific in 1996. The diameter of its dense cirrus cloud shield was less than 100 n mi (185 km) (Fig. 16), and its satellite-observed eye diameter was only 7 n mi (13 km). As with many very small TCs, the intensity forecasts erred on the low side: on the first eight warnings (issued at 6-h intervals from 0000 UTC 23 August to 1800 UTC 24 August), the 24-h intensity was underforecast by 5–25 kt; and the 48-h intensity was underforecast by as much as 30 kt (15 m s^{-1}).

Relatively few TCs in the western North Pacific first attain typhoon intensity poleward of 30°N. During the 25-yr period 1970–94 only 31 of 729 TCs (4%) that formed in the western North Pacific first attained 65 kt (33 m s^{-1}) intensity at, or north of, 25°N; only twelve at, or north of, 30°N; and only one north of 35°N. Piper reached 65 kt (33 m s^{-1}) intensity at 34°N. It remained a minimal typhoon for approximately 9 h, then fell below typhoon intensity after crossing 36°N. The SST at the point where Piper's intensity peaked was approximately 25°C (Fig. 17). Piper persisted as a well-defined TC with an intensity of 60 kt (31 m s^{-1}) as it passed 40°N, where the SST was only 20°C.

6) SUPER TYPHOON YATES (28W) AND TYPHOON ZANE (29W)

Like Tom (25W) and Violet (26W) before them, Yates and Zane moved on adjacent recurving tracks (Fig. 18). Unlike Tom and Violet, the motion of Yates and Zane possessed some characteristics of TC interaction. Note the initial cyclonic rotation of the bearing from Yates to Zane, followed by a period of anticyclonic rotation; then, as Yates recurved, the change of bearing was once again cyclonic (see inset of Fig. 18). Although these two TCs approached to within 780 n mi (1450 km) [the threshold distance noted by Brand (1970) for cyclonic change of bearing to dominate the motion of two adjacent TCs], there is little evidence that during Yates and Zane's periods of cyclonic rotation of bearing that the TCs were mutually advecting each other in a direct TC interaction. In Carr and Elsberry (1994), there are three basic kinds of TC interactions: 1) direct (a centroid-relative cyclonic orbit resulting from the TCs being advected by each other's outer winds), 2) semidirect (a centroid-relative cyclonic orbit resulting from the alteration by one TC of the steering flow between the other TC and the subtropical ridge), and 3) indirect (a centroid-relative anticyclonic change of bearing resulting from the establishment of a ridge between the two TCs). Yates and Zane had motion characteristics suggestive of all three modes of TC interaction. The steady anticyclonic change of bearing of Yates from Zane during the period 23–26 September (manifested in a south-of-west track for Yates) is typical of indirect TC interaction. The periods of cyclonic change of bearing at the beginning and at the end of the tracks are consistent with both semidirect and direct TC interaction. It is sometimes difficult to differentiate between semidirect and direct TC interaction. True mutual interaction of two TCs usually occurs when the TCs are within 780 n mi (1450 km) of each other (Brand 1970). Yates and Zane were at this threshold, and it is possible they may have interacted directly, especially at the end of their tracks when the rate of cyclonic change of bearing increased suddenly.

Tropical cyclone interaction often results in complicated forecast scenarios. While both Yates and Zane were moving toward the northwest, it was unclear which of the two would recurve first (Fig. 19). Zane had been gaining latitude faster than Yates, and (though once south of Yates) it moved so as to be at a higher latitude. When Zane slowed near Okinawa, Yates turned to the north, accelerated, and moved to a higher latitude relative to Zane. Yates then recurved ahead of Zane.

7) SUPER TYPHOON DALE (36W)

A strong equatorial westerly wind burst accompanied by unusually low equatorial sea level pressure occurred as Dale formed. After becoming a typhoon, Dale passed close to Guam where it was observed by Guam's NEXRAD. Dale produced a rare episode of phenomenal surf on the west side of Guam.

While Dale and Ernie (37W) were forming at low latitude in the western North Pacific, the sea level pressure throughout Micronesia steadily fell. Even along the

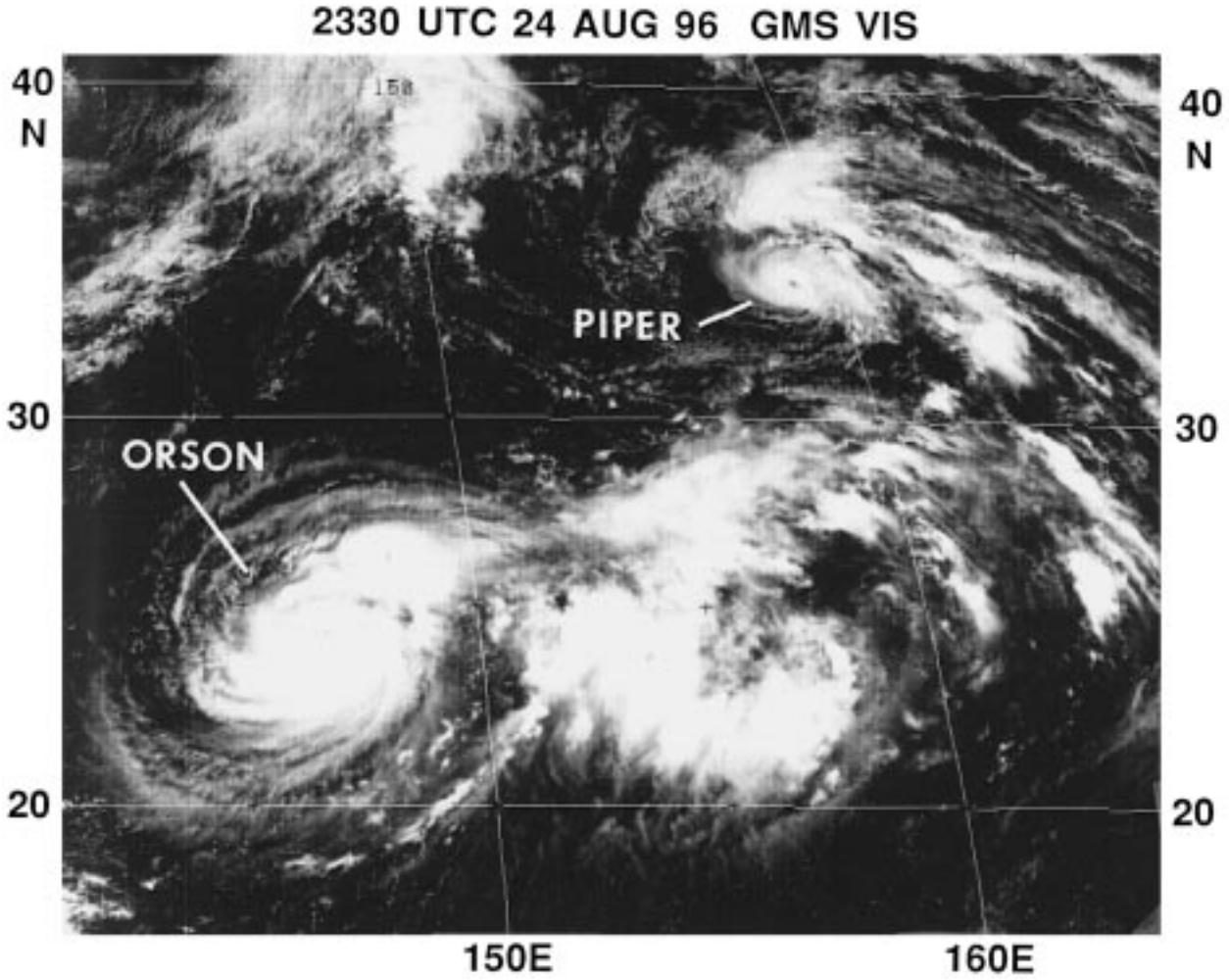

FIG. 16. The very small size of Typhoon Piper—at its peak intensity of 65 kt (33 m s^{-1})—is readily apparent when it is compared with the larger Typhoon Orson.

equator, to the south of the developing Dale, the sea level pressure steadily fell to extraordinarily low values (Figs. 20 and 21). On 4 November, several ships near the equator reported sea level pressures of 1002 hPa, or less. Values of sea level pressure this low are rarely seen along the equator. Morrissey (1990) examined the sea level pressure reports of ships within two degrees of the equator along a principal north–south shipping lane between 148° and 152°E. The ship reports used by Morrissey were extracted from the Comprehensive Ocean–Atmosphere Data Set (COADS) for an 80-yr (1900–79) period. From his analysis (Fig. 22), it is seen that few, if any, sea level pressure reports below 1004 hPa are found along the equator in this region. Ironically, approximately 10 days after the very low sea level pressure readings (and after Dale had exited the Tropics), the equatorial sea level pressure and the sea level pressure throughout Micronesia rose to exceedingly high values. The sea level pressure of 1013.5 hPa on the equator on 14 November was, according to Fig. 22, as high as the sea level pressure ever gets there. The very low sea level pressure readings, and the subsequent large rise of the sea level pressure at the equator in the western North Pacific during the life of Dale were extraordinary events.

On the night of 7 November, Dale passed 110 n mi (205 km) to the south of Guam. Guam experienced the peripheral rainbands of Dale, but never entered the eyewall cloud. For much of the time during Dale's closest point of approach, Guam remained within a dry wedge between the outer rainbands and the eyewall cloud. The air was laden with salt spray and some light rain, which allowed the NEXRAD to obtain a deep vertical profile of the wind velocity (Fig. 23). The highest winds of approximately 100 kt (51 m s^{-1}) persisted in a layer between about 6000 and 12 000 ft. At the gradient level (3000 ft), the NEXRAD showed winds of approximately 75 kt (39 m s^{-1}), which correlated well with the peak gusts observed on Guam (Fig. 24). Guam's NEXRAD has often shown that the maximum winds in a TC are

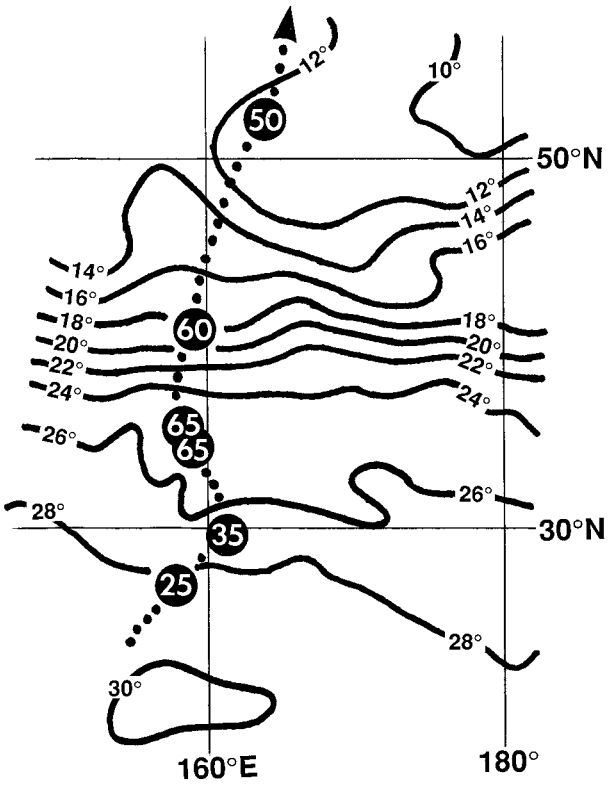

FIG. 17. Piper reached typhoon intensity at an unusually high latitude and over relatively cool SST. Intensities (kt) at selected locations are indicated by the white numbers inside the black dots. (SST contours are based upon the 0000 UTC 22 Aug navy NOGAPS analysis.)

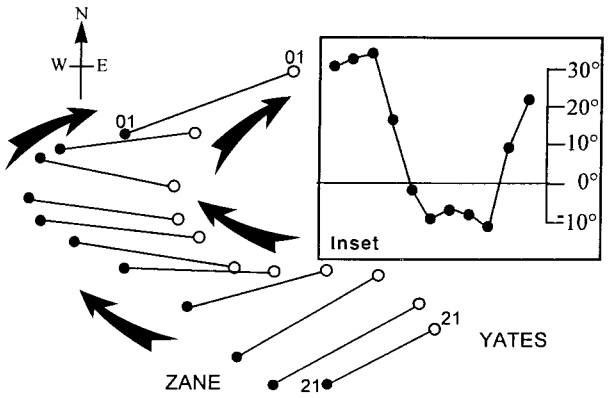

FIG. 18. A schematic illustration of the similarly shaped and spatially proximate recurving tracks of both Yates and Zane. Thin lines connect the positions of the TCs at 24-h intervals beginning at 0000 UTC 21 Sep and ending at 0000 UTC 1 Oct. The inset shows the bearing of Yates from Zane at 24-h intervals during the same time period (positive values indicate Yates north of Zane).

at the gradient level, or lower; but in Dale they were at a considerably higher altitude. Perhaps the lack of deep convection and heavy rain were factors in the relatively elevated wind maximum during Dale's closest point of approach to Guam.

After Dale passed Guam, a very large swell of 20–30 ft pounded the western shores of Guam for two days. The wave runup overtopped the 100-ft (30 m) sea cliffs of Orote Point on the west side of Guam (Fig. 25). While phenomenal surf is common on the eastern shores of Guam when typhoons pass to the south of the island, it is rare for a typhoon to produce phenomenal surf on the west side of Guam (an artifact of the usual westward movement of typhoons in the Guam area).

It is hypothesized that in order for a typhoon to generate phenomenal westerly swell on Guam it must be either very strong—in the strict sense of the meaning TC strength is defined by the average wind speed of the surrounding low-level wind flow measured within a one to three degree annulus of the center (Weatherford and Gray 1985)— and/or it must be accompanied by a large region of monsoonal gales extending to its south and west. Dale was both very strong and also possessed an extensive region of monsoon gales to its southwest. The only other typhoon in recent years—Andy (1982)—that was known to have produced phenomenal surf on Guam's western shores was accompanied by a large region of monsoon gales to its southwest. Another phenomenal surf event on the west side of Guam was not produced by a typhoon, but by persistent southwesterly monsoonal gales that were associated with a monsoon gyre in the Philippine Sea in 1974.

8) TROPICAL STORM GREG (43W)

Greg merits attention for its unusual eastward motion at low latitude and for demonstrating the importance of the microwave spectral window to accurately portray TC structure and to help derive estimates of intensity.

Greg's persistent east-southeastward motion from 8°N, 110°E to 3°N, 126°E was very unusual. TCs that form within (or move into) the SCS late in the year are often blocked from moving west by well-established northeast monsoonal flow. Such TCs often remain quasi stationary or move southwestward and dissipate. Greg formed in the SCS when a belt of low-level westerly winds existed in equatorial latitudes between monsoon troughs on either side of the equator. With the northeast monsoon blocking its motion to the west, it is hypothesized that the strong westerly winds to the south of Greg provided the flow asymmetry responsible for its eastward motion. This factor, plus the presence of the large circulation of Fern (42W) to Greg's northeast were cited on JTWC's prognostic reasoning messages as possible sources of the east-southeastward steering of Greg.

During the night of 24 December, as Greg (then TD 43W) was moving east-southeastward toward the northern tip of Borneo, a Defense Meteorological Satellite Program (DMSP) satellite passed over the system at 1452 UTC. Microwave imagery from this pass (Fig. 26) indicated that a well-organized curved band of deep convection accompanied the low-level circulation center. DMSP passes outside of the range of the Guam

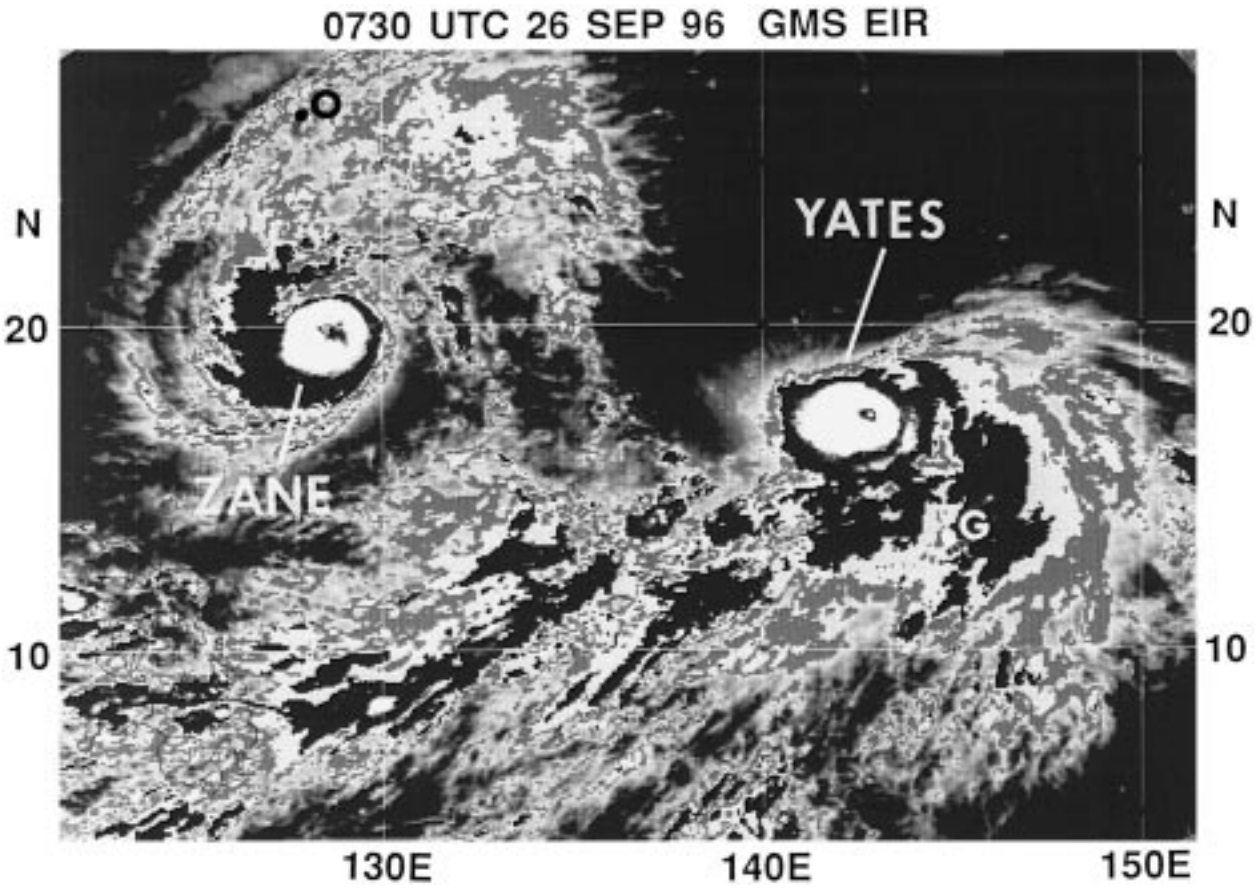

FIG. 19. Yates and Zane are both traveling toward the west-northwest in the western North Pacific. At this time it was unclear which of the TCs would be the first to recurve. Interactions between the TCs greatly complicated the track forecasts: G = Guam; O = Okinawa.

ground station are received several hours late at the JTWC via link from navy sources in Monterey, California. Though received late, the microwave imagery was nevertheless used to help support the real-time up-

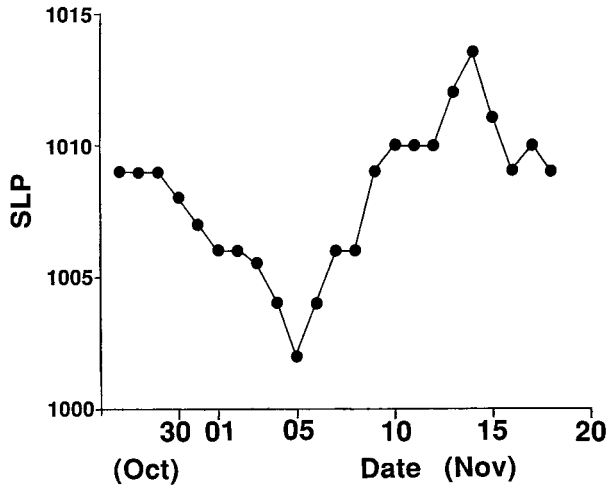

FIG. 20. Time series of the equatorial sea level pressure (SLP) (hPa) near 150°E based on ship observations.

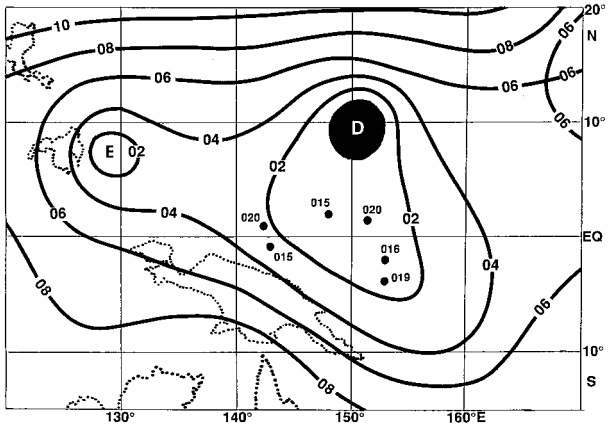

FIG. 21. SLP analysis based on a composite of ship observations at 0600 and 1800 UTC 4 Nov. Individual ships near the equator with reports of 1002 hPa or lower are indicated by dots. (D = Dale, E = Ernie, SLP contours are drawn at 2-hPa intervals, and black region indicates SLP below 1000 hPa.)

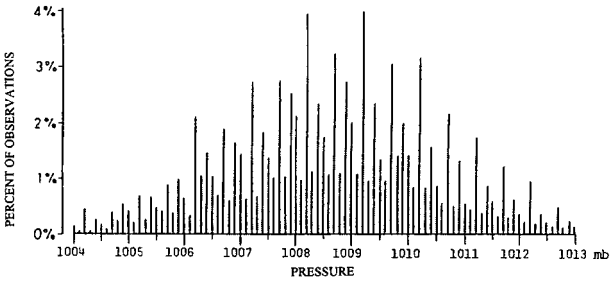

FIG. 22. Histogram of ship SLP (hPa) reports extracted from the COADS dataset in the box bounded by 2°N and 2°S from 148° to 152°E (adapted from Morrissey 1990).

grade of Greg to a tropical storm at 0000 UTC 25 December. Microwave imagery, scatterometer-derived marine surface winds, and water-vapor derived upper-level winds have seen ever-increasing application at the JTWC to the problems of TC analysis and forecasting.

3. North Indian Ocean annual summary (January–December 1996)

Because the time series of TC occurrence in the various basins has become a topic of scientific and popular interest (e.g., see Lighthill et al. 1994), JTWC statistics for the North Indian Ocean are provided for reference. Some differences exist between the JTWC totals and those reported by the New Delhi Regional Specialized Meteorological Center (RSMC). Discrepancies also exist in the best-track intensities and positions of TCs.

Tropical cyclones in the North Indian Ocean (especially in the Bay of Bengal) have been some of the deadliest in history. The Bay of Bengal, particularly the low-lying Ganges River delta region of Bangladesh, is the most dangerous TC basin in the world in terms of storm surge. One of the world's worst disasters occurred in 1970 when 300 000 lives were lost when a powerful TC made landfall there. A similar TC struck the coastal regions of Bangladesh during April 1991 and devastated the coastal city of Chittagong with winds >130 kt (67 m s^{-1}) and a 20-ft (6 m) storm surge. The official death toll in 1991 was estimated at 138 000 and the damage at U.S. $1.5 billion.

a. Annual statistics and the large-scale circulation

During 1996, eight significant TCs occurred in the North Indian Ocean. Five of these were in the Bay of

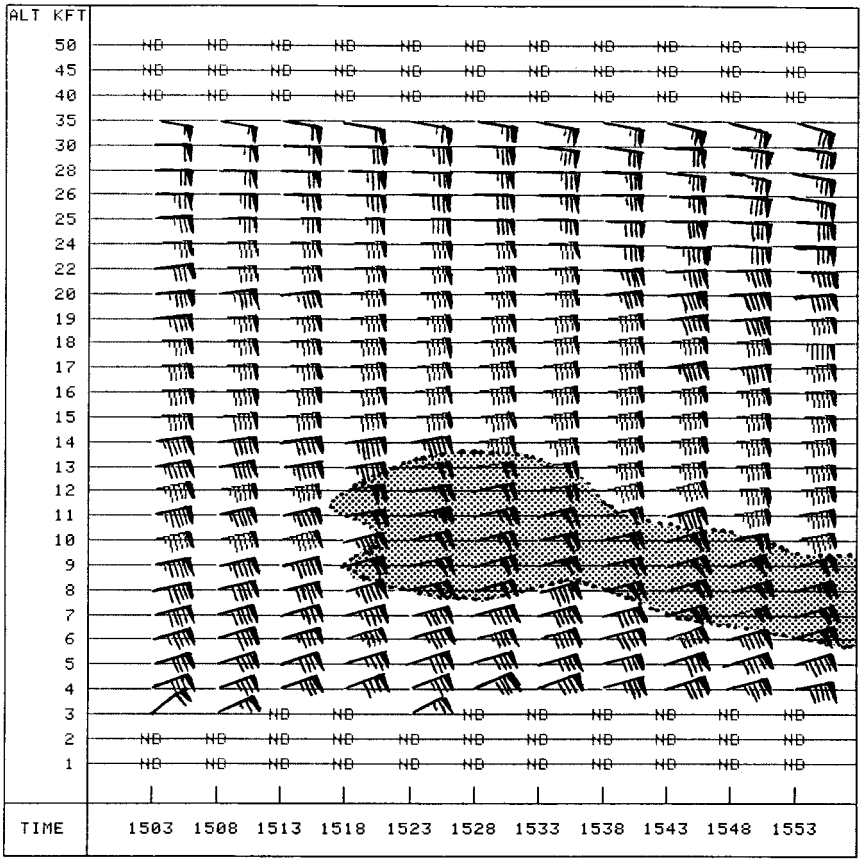

FIG. 23. A time series of the NEXRAD velocity azimuth display (VAD) wind profile near the time of Dale's closest point of approach to Guam showing wind speed of 100 kt (51 m s^{-1}) or more between 6000 and 12 000 ft (shaded region) (1553 UTC 7 Nov VAD wind profile product).

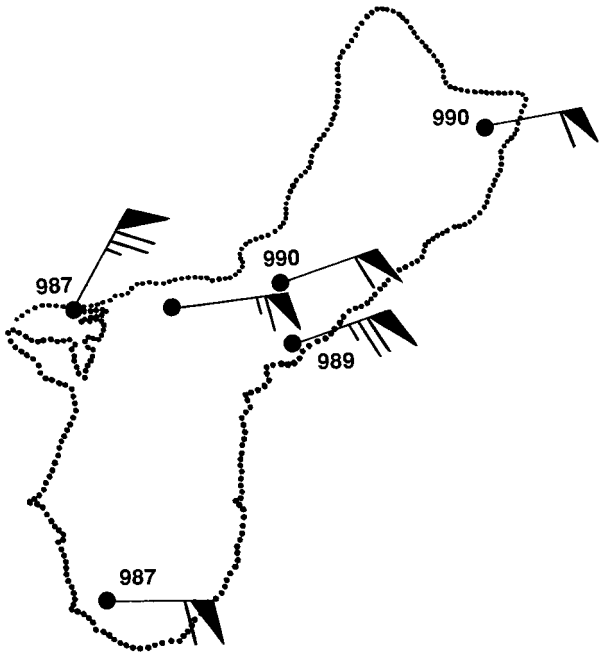

FIG. 24. Peak gusts and minimum SLP (hPa) recorded at several sites on Guam during Dale's passage.

Bengal and three in the Arabian Sea (Table 2). Spring and fall in the North Indian Ocean are periods of transition for the monsoons, and the most favorable seasons for TC activity. This year was no exception. The total number, eight, was three more than the JTWC 22-yr average of five. Eight also tied with the total in 1987; however, 1992 still holds the record at 13.

The large-scale climate (e.g., SST, low-level wind flow, distribution of deep convection) were near normal in the North Indian Ocean throughout much of 1996. During the months of peak TC activity—notably June and October—enhanced deep convection appeared over the Arabian Sea during June (Climate Prediction Center 1996), along with stronger than normal low-level monsoonal westerlies in low latitudes and increased deep convection over the Bay of Bengal and Indonesia during October.

b. Noteworthy tropical cyclones

1) TROPICAL CYCLONE (TC) 01B

During May 1996, TC 01B originated in the Bay of Bengal in association with an equatorial westerly wind burst. In the Southern Hemisphere, a ''twin'' TC (Lander 1990)—TC 28S (Jenna)—developed in conjunction

FIG. 25. Seawater explodes 100 ft into the air as a wave reflecting off the Orote Point, Guam, cliff line meets an oncoming breaker (photo courtesy of Major R. Edson).

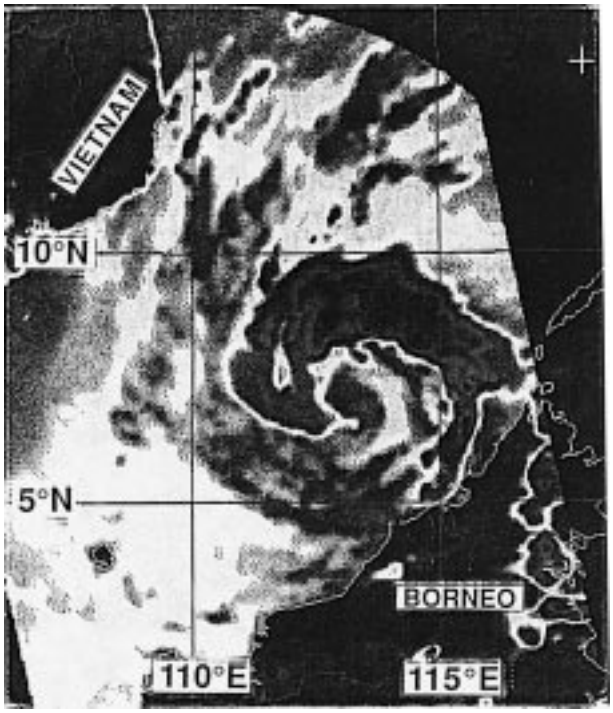

FIG. 26. A well-defined spiral band of deep convection, wrapping almost one complete turn from tip to tail around Greg's low-level circulation center, helped to support the postanalysis timing (and warning upgrade) of TD 43W to TS intensity (1452 UTC 24 Dec horizontally polarized 85-GHz Special Sensor Microwave Imager DMSP imagery).

with the same equatorial westerly wind burst. Fortunately, TC 01B was weak, reaching a peak intensity of only 40 kt (21 m s^{-1}) shortly before making landfall near Cox's Bazar, Bangladesh. No reports of death or significant damage were received at the JTWC.

2) TROPICAL CYCLONE (TC) 04A

During mid-June 1996, TC 04A originated from a monsoon depression that was initially detected off the west coast of India 390 km south-southwest of Bombay. Moving generally northward, the system became a minimal hurricane and made landfall near Diu (located on the northwestern coast of India 610 km southeast of Karachi, Pakistan). The maximum storm surge at landfall was estimated to be 20 ft (6 m). Indian government agencies reported 47 people were killed by the cyclone.

3) TROPICAL CYCLONE (TC) 06B

Originating during late October from a tropical disturbance near the Andaman Islands in the Bay of Bengal, TC 06B intensified, recurved, and made landfall on the heavily populated delta region of West Bengal, India, near the Bangladesh border. Heavy rains associated with this TC caused flooding that immobilized much of metropolitan Calcutta. A 9-ft (3 m) storm surge inundated low-lying coastal areas in Bangladesh where reports indicated that 14 people were killed, over 2000 people were injured, and 100 fishermen were missing

4) TROPICAL CYCLONE (TC) 07B

During early November 1996, TC 07B began as a weak low pressure area in the Andaman Sea. Traveling westward across the Bay of Bengal, the system intensified more rapidly than the normal rate of one T number per day (Dvorak 1975) and peaked at 115 kt (59 m s^{-1}) just before landfall on the west coast of India near Kakinada (445 km northeast of Madras). The impact of this cyclone in coastal areas was significant. More than 1000 fisherman were reported missing at sea, and 42 passengers were lost when a ferry sank. TC 07B was also responsible for widespread flooding, the destruction of at least 10 000 homes, and the loss of hundreds of thousands of acres of rice crop. More than 250 villages were reported under water and many coastal communities were inundated by 12-ft (4 m) waves.

4. Southern Hemisphere annual summary (July 1995–June 1996)

As in the Indian Ocean, some differences exist between the JTWC totals and the totals reported by RSMCs covering the Southern Hemisphere. Discrepancies also exist in the best-track intensities and positions.

The total number of significant TCs during the 1996 Southern Hemisphere season (1 July 1995–30 June 1996) was 28, which was slightly more than the overall climatological mean of 27.3 for the previous 16 years. Of these 28 significant TCs there were 16 of hurricane intensity, 11 tropical storms, and one tropical depression (Table 3). By subregions (South Indian, west of 105°E; Australian, 105°–165°E; South Pacific, east of 165°E), TC activity was slightly greater than normal in the South Indian Ocean and Australian regions, and slightly below normal in the South Pacific. The regional distribution of TCs in the Southern Hemisphere during 1996 was markedly similar to the TC distribution during the previous year (1995) when it was also greater in the South Indian Ocean and Australian regions and reduced in the South Pacific. During the latter half of 1995 and throughout the first half of 1996, weak ENSO cold-phase large-scale climate anomalies persisted. The westward shift of TC activity in the Southern Hemisphere may be consistent with these large-scale climatic anomalies. For the western North Pacific there is a pronounced eastward shift of the mean genesis location during El Niño years, and a pronounced westward shift of the mean genesis location during La Niña years (Chan 1985; Dong 1988; Lander 1994). A similarly pronounced ENSO-related shift in the annual-mean location of TC genesis has been shown to exist in the South Pacific (e.g., Basher 1995). During El Niño years, TC

TABLE 2. North Indian Ocean 1996 tropical cyclone statistics.

Tropical cyclone number[a]	Name[a]	Class[b]	Dates[c]	Maximum 1-min wind ($m\ s^{-1}$)	(mb)
01B	—	TS	7–8 May	21	994
02A	—	TS	11–11 Jun	21	994
03B	—	TS	12–17 Jun	23	988[d]
04A	—	TS	17–19 Jun	26	972[d]
05A	—	TS	22–31 Oct	28	984
06B	—	TS	25–29 Oct	23	991
07B	—	H	3–7 Nov	59	927
08B	—	H	28 Nov–6 Dec	39	967

[a] The numbers are according to the JTWC: A = Arabian Sea, B = Bay of Bengal. Tropical cyclones in the North Indian Ocean are not named by the New Delhi RSMC.
[b] TD: tropical depression, wind speed less than 17 m s^{-1}. TS: tropical storm, wind speed 17–32 m s^{-1}. H: hurricane, wind speed 33 m s^{-1} or higher.
[c] Dates begin at 0000 UTC and include only the period of warning.
[d] Minimum SLP for these TCs was based upon synoptic data at landfall.

TABLE 3. Southern Hemisphere 1996[f] tropical cyclone statistics.

Tropical cyclone number[a]	Name[a]	Class[b]	Dates[c]	Maximum 1-min wind ($m\ s^{-1}$)	Minimum SLP (mb)
01S	Daryl[c]	H	17–25 Nov '95	77	885
02S	Emma	TS	4–15 Dec	18	997
03S	Frank	H	7–13 Dec	59	927
04S	Gertie	H	18–21 Dec	39	967
05P	Barry	H	4–7 Jan '96	41	963
06S	Bonita	H	5–15 Jan	69	904
07S	Hubert[e]	H	8–12 Jan	39	967
08P	Yasi	TS	16–19 Jan	23	991
09P	Celeste	H	27–30 Jan	33	976
10P	Jacob	H	28 Jan–7 Feb	46	954
11S	Isobel	TS	7–9 Feb	23	991
12S	—	TS	21–26 Feb	18	997
13P	Dennis	TS	13–18 Feb	23	991
14S	Doloresse	H	15–19 Feb	39	967
15S	—	TS	16–17 Feb	18	997
16S	Edwige	H	22–29 Feb	49	949
17S	Flossy	H	27 Feb–4 Mar	59	927
18S	Kirsty	H	4–12 Mar	51	943
19P	Ethel	TS	9–13 Mar	23	991
20P	Zaka	TS	10–11 Mar	21	994
21P	Atu	TS	10–13 Mar	28	984
22S	Guylianne	TS	20–23 Mar	18	997
23P	Beti	H	21–29 Mar	54	938
24S	Hansella	H	3–10 Apr	49	949
25S	Olivia	H	5–11 Apr	64	916
26S	Itelle	H	8–17 Apr	72	898
27S	—	TD	16–19 Apr	15	1000
28S	Jenna	TS	1–6 May	31	980

[a] The numbers are according to the JTWC: P = South Pacific, S = South Indian Ocean. The names are provided by the responsible WMO-designated RSMC (e.g., La Réunion, Perth, Darwin, Brisbane, Fiji, Port Moresby).
[b] TD: tropical depression, wind speed less than 17 m s^{-1}. TS: tropical storm, wind speed 17–32 m s^{-1}. H: hurricane, wind speed 33 m s^{-1} or higher.
[c] Dates begin at 0000 UTC and include only the period of warning.
[d] Daryl was renamed Agnielle when it passed from Perth's AOR into the AOR of La Réunion.
[e] Hubert was renamed Coryna when it passed from Perth's AOR into the AOR of La Réunion.
[f] The Southern Hemisphere statistics for 1996 are compiled by the JTWC for the period Jul 1995–Jun 1996.

formation in the South Pacific is drawn eastward and equatorward. During La Niña years, TC formation in the South Pacific tends to occur farther westward and southward (i.e., closer to Australia).

5. Concluding remarks

Although 1996, like 1995, had abundant TCs in the Atlantic, and few TCs in the eastern North Pacific, the number of TCs in the western North Pacific increased dramatically from its low value during 1995. Overall, 1995 was a quiet year in the Eastern Hemisphere with a total of 52 TCs (of TS intensity or higher) versus a normal of 60. Contributing to the low number of Eastern Hemisphere TCs during 1995 was the below-normal number of TCs in the western North Pacific and the North Indian Ocean, and a well-below normal number of TCs in the Southern Hemisphere. By contrast, the number of Eastern Hemisphere TCs saw a marked increase during 1996 with a total of 69 TCs. Contributing to the increase in Eastern Hemisphere TCs was a well above-normal number of TCs in the western North Pacific and the North Indian Ocean combined with a slightly above-normal number of TCs in the Southern Hemisphere.

In retrospect, the return of near-normal mean monthly monsoonal flow to the western North Pacific during November and December of 1996 may have signaled the onset of the strong 1997 El Niño. During early November 1996 and then again in the latter half of December 1996, there occurred episodes of very strong equatorial westerly winds from Indonesia eastward to 165°E. November's equatorial west wind episode was associated with the formation of TCs Dale and Ernie in the western North Pacific. December's prolonged and strong equatorial westerly wind episode was associated with a prolific outbreak of six TCs—three in the western North Pacific and three in the Southern Hemisphere.

Acknowledgments. Support for the preparation and publication of this paper was provided by the Office of Naval Research through Grant N00014-96-1-0744. The support of the personnel at the Joint Typhoon Warning Center in allowing us access to their satellite imagery and other meteorological data is greatly appreciated. A special thanks is owed to Brian Hong for his work on the graphics, and to an anonymous reviewer who provided extensive and helpful editorial comments on the original manuscript.

REFERENCES

Basher, R. E., and X. Zheng, 1995: Tropical cyclones in the southwest Pacific: Spatial patterns and relationships to Southern Oscillation and sea surface temperature. *J. Climate,* **8,** 1249–1260.

Black, P. G, 1983: Tropical storm structure revealed by stereoscopic photographs from Skylab. *Adv. Space Res.,* **2,** 115–124.

——, and F. D. Marks Jr., 1987: Environmental interactions associated with hurricane supercells. *Proc. 17th Conf. on Hurricanes and Tropical Meteorology,* Miami, FL, Amer. Meteor. Soc., 416–419.

——, and ——, 1991: The structure of an eyewall meso-vortex in Hurricane Hugo (1989). Preprints, *19th Conf. on Hurricanes and Tropical Meteorology,* Miami, FL, Amer. Meteor. Soc., 357–358.

——, ——, and R. A. Black, 1986: Supercell structure in tropical cyclones. *Proc. 23d Conf. on Radar Meteorology,* Snowmass, CO, Amer. Meteor. Soc., JP255–JP259.

Brand, S., 1970: Interaction of binary tropical cyclones of the western North Pacific Ocean. *J. Appl. Meteor.,* **9,** 433–441.

Carr, L. E., and R. L. Elsberry, 1994: Systematic and integrated approach to tropical cyclone forecasting. Part I: Description of basic approach. Naval Postgraduate School Pub. NPS-MR-002, 65 pp. [Available from Dept. of Meteorology, Naval Postgraduate School, Monterey, CA 93943.]

Chan, J. C. L., 1985: Tropical cyclone activity in the northwest Pacific in relation to the El Niño/Southern Oscillation phenomenon. *Mon. Wea. Rev.,* **113,** 599–606.

Climate Prediction Center (CPC), 1996: *Climate Diagnostics Bulletin.* Vol. 96, Nos. 1–12. [Available from U.S. Dept. of Commerce, Washington, DC 20233.]

Dong, K., 1988: El Niño and tropical cyclone frequency in the Australian region and the northwest Pacific. *Aust. Meteor. Mag.,* **36,** 219–255.

Dunnavan, G. M., 1981: Forecasting intense tropical cyclones using 700 mb equivalent potential temperature and central sea-level pressure. NOCC/JTWC Tech. Note 81-1, 12 pp. [Available from Joint Typhoon Warning Center, 425 Luapele Rd., Pearl Harbor, HI 96860.]

Dvorak, V. F., 1975: Tropical cyclone intensity analysis and forecasting from satellite imagery. *Mon. Wea. Rev.,* **103,** 420–430.

——, 1984: Tropical cyclone intensity analysis using satellite data. NOAA Tech. Rep. NESDIS 11, 46 pp. [Available from NOAA/NESDIS, Washington, DC 20233.]

Hebert, P. H., and K. O. Poteat, 1975: A satellite classification technique for subtropical cyclones. NOAA Tech. Memo. NWS SR-83, 25 pp. [Available from National Weather Service, Fort Worth, TX 76102.]

Japan Meteorological Agency (JMA), 1976: The north-oriented track type. Forecasting Manual for Typhoons (in English), 227 pp. [Available from Japan Meteorological Agency, 1-3-4 Ote-machi, Chiyoda-ku, Tokyo, Japan.]

JTWC, 1960: Typhoon Carmen. 1960 Annual Typhoon Report, 219 pp. [NTIS AD 786147.]

——, 1994: Typhoon Seth. Annual Tropical Cyclone Report, 337 pp. [NTIS AD A301618.]

Lander, M. A., 1990: Evolution of the cloud pattern during the formation of tropical cyclone twins symmetrical with respect to the equator. *Mon. Wea. Rev.,* **118,** 1194–1202.

——, 1994: An exploration of the relationships between tropical storm formation in the western North Pacific and ENSO. *Mon. Wea. Rev.,* **122,** 636–651.

Lighthill, J., G. J. Holland, W. M. Gray, C. Landsea, G. Craig, J. Evans, Y. Kurihara, and C. P. Guard, 1994: Global climate change and tropical cyclones. *Bull. Amer. Meteor. Soc.,* **75,** 2147–2157.

Marks, F. D., Jr., and R. A. Houze Jr., 1984: Airborne Doppler radar observations in Hurricane Debby. *Bull. Amer. Meteor. Soc.,* **65,** 569–582.

Merrill, R. T., 1984: A comparison of large and small tropical cyclones. *Mon. Wea. Rev.,* **112,** 1408–1418.

Miller, D. W., and M. A. Lander, 1997: Intensity estimation of tropical cyclones during extratropical transition. JTWC/SATOPS Tech. Note 97-002. [Available from the Joint Typhoon Warning Center, 425 Luapele Rd., Pearl Harbor, HI 96860.]

Morrissey, M. L., 1990: An evaluation of ship data in the equatorial Pacific. *J. Climate,* **3,** 99–112.

Rasmusson, E. M., and T. H. Carpenter, 1982: Variations in tropical sea surface temperature and surface wind fields associated with the Southern Oscillation/El Niño. *Mon. Wea. Rev.,* **110,** 354–384.

Ropelewski, C. F., and M. S. Halpert, 1987: Global and regional precipitation patterns associated with the El Niño/Southern Oscillation. *Mon. Wea. Rev.*, **115,** 1606–1626.

Sadler, J. C., 1967: The tropical upper tropospheric trough as a secondary source of typhoons and a primary source of trade wind disturbances. Final Rep. AF 19(628)-3860 HIG Rep. 67-12, 44 pp. [Available from Hawaii Institute of Geophysics, 2525 Correa Rd., University of Hawaii, Honolulu, HI 96822.]

——, 1976: A role of the tropical upper tropospheric trough in early season typhoon development. *Mon. Wea. Rev.*, **104,** 1266–1278.

——, 1978: Mid-season typhoon development and intensity changes and the tropical upper tropospheric trough. *Mon. Wea. Rev.*, **106,** 1137–1152.

——, M. A. Lander, A. M. Hori, and L. K. Oda, 1987: Pacific Ocean. Vol. 2, Tropical Marine Climatic Atlas. UHMET Pub. 87-02, 14 pp. [Available from Department of Meteorology, University of Hawaii, Honolulu, HI 96822.]

Stewart, S. R., and S. W. Lyons, 1996: A WSR-88D radar view of Tropical Cyclone Ed. *Wea. Forecasting*, **11,** 115–135.

——, J. Simpson, and D. Wolff, 1997: Convectively-induced mesocyclonic vortices in the eyewall of tropical cyclones as seen by WSR-88D doppler radars. Preprints, *22d Conf. on Hurricanes and Tropical Meteorology*, Fort Collins, CO, Amer. Meteor. Soc., 106–108.

Trenberth, K. E., 1997: The definition of El Niño. *Bull. Amer. Meteor. Soc.*, **78,** 2771–2777.

Wakimoto, R. M., and P. G. Black, 1993: Damage survey of Hurricane Andrew and its relationship to the radar-detected eyewall. *Proc. 20th Conf. on Hurricanes and Tropical Meteorology*, San Antonio, TX, Amer. Meteor. Soc., 54–57.

Weatherford, C. L., and W. M. Gray, 1985: Typhoon structural variability. Colorado State University Department of Atmospheric Science Paper 391, 77 pp. [Available from Dept. of Atmospheric Science, Colorado State University, Fort Collins, CO 80523.]

Zehr, R. M., 1992: Tropical cyclogenesis in the western North Pacific. NOAA Tech. Rep. NESDIS 61, 181 pp. [Available from NOAA/NESDIS, RAMM Branch, Colorado State University, Fort Collins, CO 80523.]